
# WP6 Report

# Interactions with structures

# ANNEX

**WP Responsible:** PP9 – University of Ljubljana, Faculty of Civil and Geodetic Engineering, Slovenia
**Coordination:** Jošt Sodnik

**Contributors:**

| | |
|---|---|
| LP | BMLFUW - Federal Ministry of Agriculture, Forestry, Environment and Water Management, Dep. IV/5 Torrent and Avalanche |
| PP3 | UNI PD TESAF - University of Padova-Department Land, environment, Agriculture and Forestry |
| PP5 | Piedmont Region |
| PP7 | IRSTEA Grenoble, Snow avalanche engineering and torrent control research unit |
| PP9 | UL FGG - University of Ljubljana, Faculty of Civil and Geodetic Engineering |
| PP11 | BOKU - University of Natural Resources and Life Sciences Vienna, Institute for Water Management, Hydrology and Hydraulic Engineering, Dep. Water-Atmosphere-Environment |

# Contents

# 5 Annex

## 5.1 A physical scale model to investigar torrential filter structures

Markus Moser, Gerald Jäger, Susanne Mehlhorn - BMLFUW

### 5.1.1. Planning approach – Model Setup

Two different types of check dams are investigated. A screen-dam with inclined vertical beams is compared with a beam-dam with horizontal beam. The experiments should evaluate the variation of sediment transport of these structures including the influence of coarse woody debris. Therefore the distance between the steel elements can be adjusted to show their ability to filter sediment. The distances have been varied from 10.5 mm (=$d_{90}$ of the grain-size distribution) to 15 mm. The physical scale of the experiments is 1:30. All experimental runs are Froude scaled. Both dams are tested in elongated and pear-shaped sediment retention basins in order to investigate the shape effect of the deposition area. Both different geometries are shown in Figure 1 and Figure 2. The inclination of the basin is 5 %.

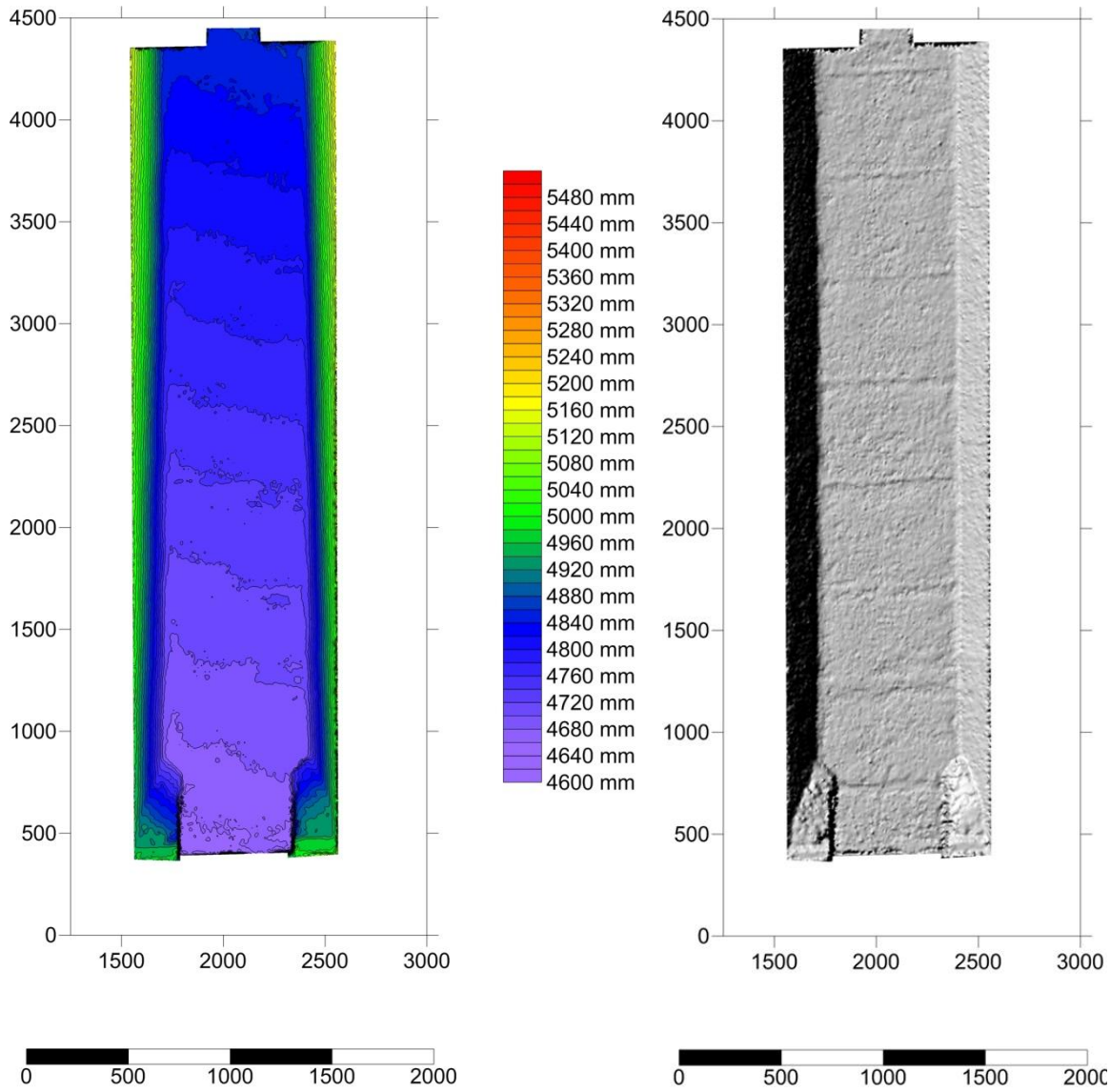


**Figure 1: Elevation model and hill-shade of the elongated deposition basin.**

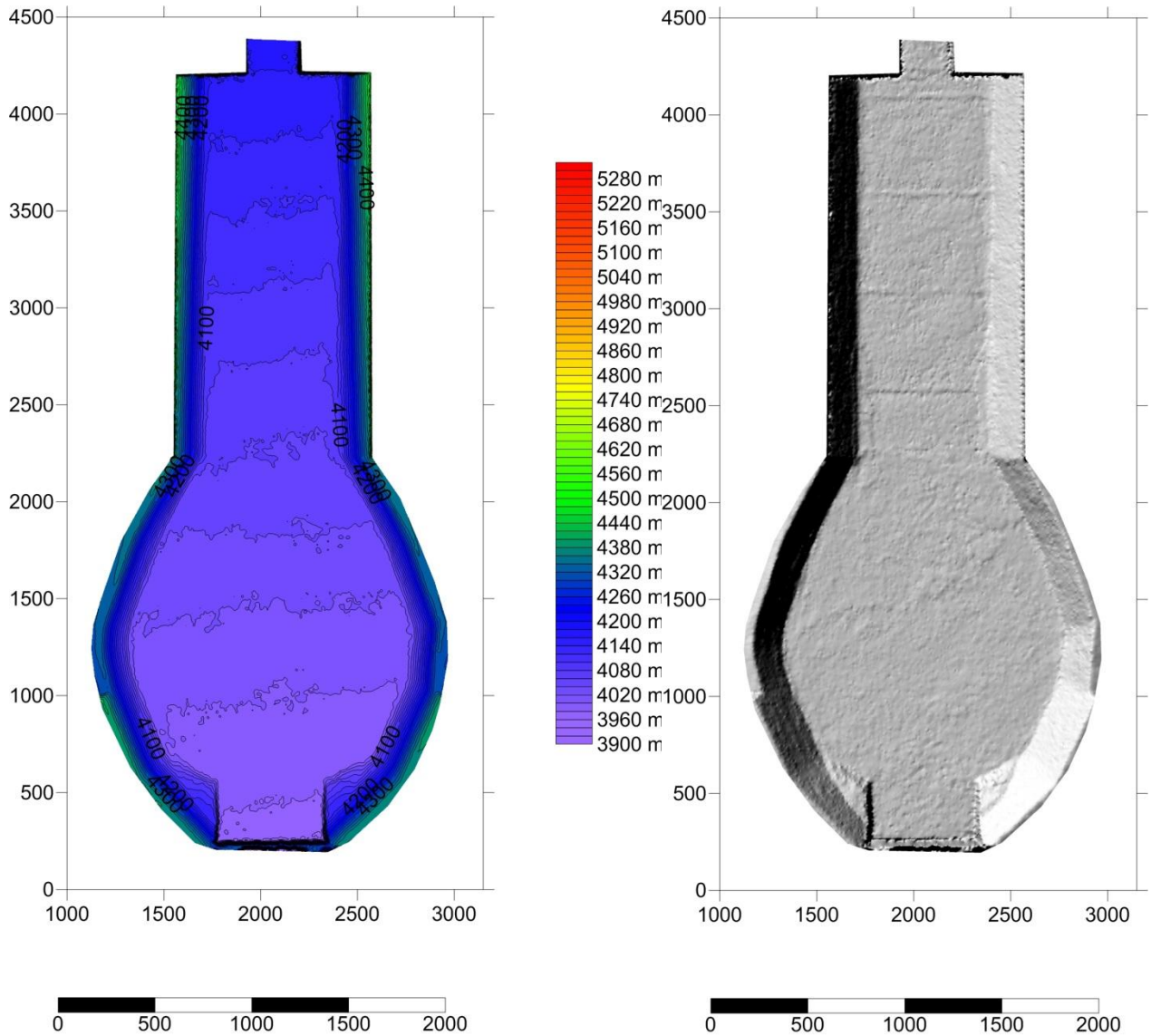


**Figure 2: Elevation model and hill-shade of the pear-shaped deposition basin.**

### 5.1.2 Experiments

First the hydraulic effect of the structures is investigated by measuring the flow field and the back-water effects of the protection measures. For a systematic comparison of the two check dams experiments with fluvial bedload transport are made. First a typical hydrograph for an extreme flood ($HQ_{150}$) with unlimited sediment supply is modelled. Therefore a typical torrential sediment mixture with a wide grain-size distribution is used. The sediment is fed by a conveyor belt according the transport capacity of the upstream reach. A total sediment volume of 1.05 m³ is needed for each run. Then the deposition is scanned with a 2-D laser-scan device mounted on a rail above the basin in order to analyse the deposition pattern and the deposited volume. Afterwards a flood with a lower reoccurrence period ($HQ_5$) without sediment transport from upstream is modelled to investigate the ability of the protection structure for self-emptying. Then the basin is scanned again to quantify the volume change in the deposition basin.

To investigate the influence of driftwood on the deposition behaviour experiments with logs are made. The hydro- and sedigraphs are the same as described above, but different

log diameters and lengths are added upstream the basin. After scanning the surface the driftwood is removed carefully to model the cleaning of a log jam. An Example of a log jam can be seen in Figure 3. The view from the other side is shown in Figure 4. Then the more frequent flood without sediment and wood from upstream is modelled to show the self-emptying behaviour of the basins.

**Figure 3: Example of a log jams caused by the added driftwood for both types of dams.**

**Figure 4: Rear view of log jams caused by the added driftwood for both types of dams.**

An overview of all model runs for the elongated basin is shown in Table 1 and for the pear-shaped basin in Table 2. Each run consists of the HQ150 and HQ5 design event. Clearwater means that only the hydraulic behaviour (e.g. backwater effects of the dam in the basin) was investigated. Bedload means that 1,05 m³ of bedload material were added by a conveyor belt according the transport capacity of the upstream reach. And finally driftwood means that during the HQ150 event additionally to the bedload driftwood was fed manually according a fixed timetable.

**Table 1: Overview of the experimental runs for the elongated basin. Each run consist of the HQ150 and HQ5 design event.**

| Nr. | Type | Beam distance | Clear water | Bedload | Driftwood |
|---|---|---|---|---|---|
| 001 | screen dam | 10,5 mm | | ■ | |
| 002 | screen dam | 10,5 mm | | ■ | ■ |
| 003 | screen dam | 15 mm | | ■ | ■ |
| 004 | screen dam | 15 mm | | ■ | |
| 005 | screen dam | 15 mm | ■ | | |
| 006 | beam dam | 10,5 mm | | ■ | |
| 007 | beam dam | 10,5 mm | | ■ | ■ |
| 008 | beam dam | 15 mm | | ■ | ■ |
| 009 | beam dam | 15 mm | ■ | | |
| 010 | beam dam | 15 mm | | ■ | |

**Table 2: Overview of the experimental runs for the pear shaped basin. Each run consist of the HQ150 and HQ5 design event.**

| Nr. | Type | Beam distance | Clear water | Bedload | Driftwood |
|---|---|---|---|---|---|
| 011 | screen dam | 15 mm | | ■ | |
| 012 | screen dam | 15 mm | | ■ | ■ |
| 013 | screen dam | 15 mm | ■ | | |
| 014 | screen dam | 10,5 mm | | ■ | ■ |
| 015 | screen dam | 10,5 mm | | ■ | |
| 016 | beam dam | 15 mm | | ■ | |
| 017 | beam dam | 15 mm | | ■ | ■ |
| 018 | beam dam | 15 mm | ■ | | |
| 019 | beam dam | 10,5 mm | ■ | | |
| 020 | beam dam | 10,5 mm | | ■ | |
| 021 | beam dam | 10,5 mm | | ■ | ■ |

### 5.1.3 Data Analysis

#### 5.1.3.1 Deposition and erosion pattern

After each experiment the deposition was scanned by a laser-scan device mounted above the basin. With the known geometry of the basin the volume in the deposition basin was calculated by subtracting the elevation models after the $HQ_{150}$ and $HQ_5$. An example of a scan of a deposition for the experimental run Nr. 15 (screen dam with 10,5 mm beam distance and bedload transport without driftwood) is shown in Figure 5. The $HQ_5$ transported only sediment that was already deposited in the basin and some sediment that deposited in the channel upstream the basin. The deposition (left) and erosion (right) pattern can be seen in the hills-hade figures below.

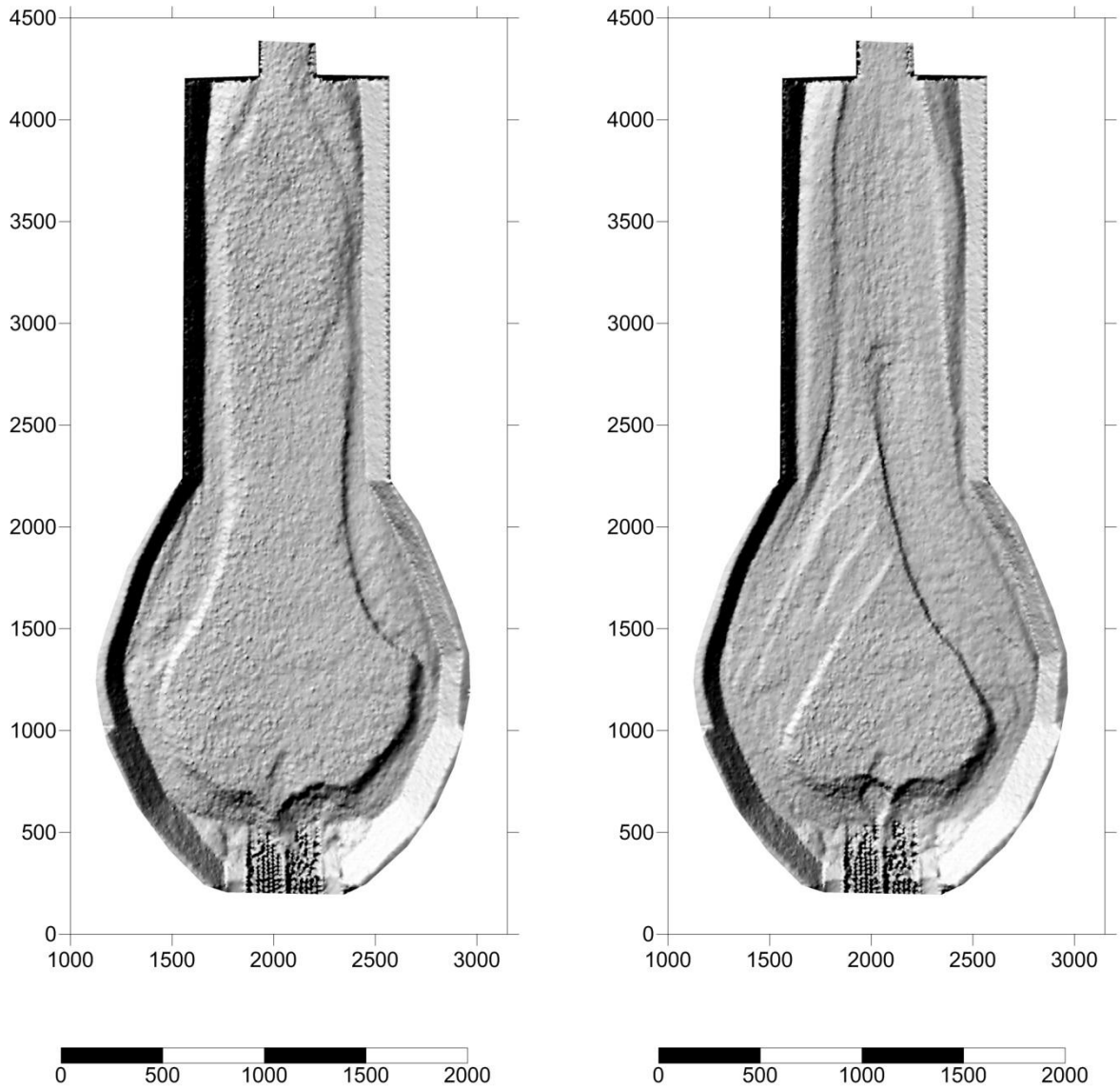


**Figure 5: Hill-shade of the pear-shaped deposition basin for the experimental run 15 after the HQ150 event with bedload transport and the following HQ5 event without additional bedload from upstream.**

5.1.3.2 Deposition volumes

Table 3 shows an overview of the deposition volumes for the elongated basin. The basin has been scanned after the $HQ_{150}$ event and finally after the following $HQ_5$ event. Table 4 shows an overview of the deposition volumes for the pear shaped basin for the same setup.

**Table 3: Overview of the deposition volumes for the elongated basin. Each run consist of the HQ150 and is followed by a HQ5 design event.**

| Nr. | Type | Beam distance | Clear water | Bedload | Driftwood | Deposition [m³] | |
|---|---|---|---|---|---|---|---|
| | | | | | | HQ 150 | HQ 5 |
| 001 | screen dam | 10,5 mm | | | | 0,5213 | 0,5524 |
| 002 | screen dam | 10,5 mm | | | | 0,6018 | 0,7125 |
| 003 | screen dam | 15 mm | | | | 0,3398 | 0,2917 |
| 004 | screen dam | 15 mm | | | | 0,2421 | 0,2476 |
| 005 | screen dam | 15 mm | | | | - | - |
| 006 | beam dam | 10,5 mm | | | | 0,5879 | 0,6375 |
| 007 | beam dam | 10,5 mm | | | | 0,6203 | 0,7216 |
| 008 | beam dam | 15 mm | | | | 0,5417 | 0,4138 |
| 009 | beam dam | 15 mm | | | | - | - |
| 010 | beam dam | 15 mm | | | | 0,1879 | 0,1789 |

**Table 4: Overview of the deposition volumes for the pear shaped basin. Each run consist of the HQ150 and is followed by a HQ5 design event.**

| Nr. | Type | Beam distance | Clear water | Bedload | Driftwood | Deposition [m³] | |
|---|---|---|---|---|---|---|---|
| | | | | | | HQ 150 | HQ 5 |
| 011 | screen dam | 15 mm | | | | 0,3716 | 0,3536 |
| 012 | screen dam | 15 mm | | | | 0,4962 | 0,4023 |
| 013 | screen dam | 15 mm | | | | - | - |
| 014 | screen dam | 10,5 mm | | | | 0,6295 | 0,6278 |
| 015 | screen dam | 10,5 mm | | | | 0,5641 | 0,5852 |
| 016 | beam dam | 15 mm | | | | 0,2486 | 0,2023 |
| 017 | beam dam | 15 mm | | | | 0,4054 | 0,2773 |
| 018 | beam dam | 15 mm | | | | - | - |
| 019 | beam dam | 10,5 mm | | | | - | - |
| 020 | beam dam | 10,5 mm | | | | 0,6337 | 0,705 |
| 021 | beam dam | 10,5 mm | | | | 0,6379 | 0,7353 |

#### 5.1.3.3 Sediment passing the dam and self-emptying

The sediment volumes that passed the check-dam are given in Table 5 and Table 6. The value given in column $HQ_5$ is the total volume that passed after $Hq_{100}$ and $HQ_5$. Finally the effect of self-emptying efficiency [%] due to the $HQ_5$ was calculated by:

$$SEE = \frac{V_p - \overline{V}_p}{V_t - V_{UP}} \cdot 100$$

$SEE$ …self-emptying efficiency; $V_p$ … Total volume sediment passing

$\overline{V}_p$ …Volume sediment passing $HQ_{100}$; $V_t$ … Total sediment volume;

$V_{UP}$ …Sediment deposition in the upstream reach

**Table 5: Sediment passing the check dam self-emptying for the elongated basin.**

| Nr. | Type | Beam distance | Clear water | Bedload | Driftwood | Sediment passing [m³] | | self-emptying after HQ 5 [%] |
|---|---|---|---|---|---|---|---|---|
| | | | | | | HQ 150 | HQ 5 | |
| 1 | screen dam | 10,5 mm | | ■ | | 0,3582 | 0,4550 | 10 |
| 2 | screen dam | 10,5 mm | | ■ | ■ | 0,2777 | 0,2949 | 2 |
| 3 | screen dam | 15 mm | | ■ | ■ | 0,5397 | 0,7157 | 17 |
| 4 | screen dam | 15 mm | | ■ | | 0,6374 | 0,7598 | 12 |
| 5 | screen dam | 15 mm | ■ | | | - | - | - |
| 6 | beam dam | 10,5 mm | | ■ | | 0,2916 | 0,3699 | 8 |
| 7 | beam dam | 10,5 mm | | ■ | ■ | 0,2592 | 0,2858 | 3 |
| 8 | beam dam | 15 mm | | ■ | ■ | 0,3378 | 0,5936 | 25 |
| 9 | beam dam | 15 mm | ■ | | | - | - | - |
| 10 | beam dam | 15 mm | | ■ | | 0,6916 | 0,8285 | 14 |

**Table 6: Sediment passing the check dam self-emptying for the pear shaped basin.**

| Nr. | Type | Beam distance | Clear water | Bedload | Driftwood | Sediment passing [m³] | | self-emptying after HQ 5 [%] |
|---|---|---|---|---|---|---|---|---|
| | | | | | | HQ 150 | HQ 5 | |
| 11 | screen dam | 15 mm | | ■ | | 0,5079 | 0,6538 | 14 |
| 12 | screen dam | 15 mm | | ■ | ■ | 0,3833 | 0,6051 | 22 |
| 13 | screen dam | 15 mm | ■ | | | - | - | - |
| 14 | screen dam | 10,5 mm | | ■ | ■ | 0,2500 | 0,3796 | 13 |
| 15 | screen dam | 10,5 mm | | ■ | | 0,3154 | 0,4222 | 11 |
| 16 | beam dam | 15 mm | | ■ | | 0,6309 | 0,8051 | 17 |
| 17 | beam dam | 15 mm | | ■ | ■ | 0,4741 | 0,7301 | 25 |
| 18 | beam dam | 15 mm | ■ | | | - | - | - |
| 19 | beam dam | 10,5 mm | ■ | | | - | - | - |
| 20 | beam dam | 10,5 mm | | ■ | | 0,2458 | 0,3024 | 6 |
| 21 | beam dam | 10,5 mm | | ■ | ■ | 0,2416 | 0,2721 | 3 |

#### 5.1.3.4 Comparison of the different experimental runs

For further analyses comparable experiments were grouped to show the effect of the beam distance, shape of the deposition basin and effect of the dam type. Figure 6 shows the experiments with bedload added but without drift wood. The given volumes are the deposition in the storage area after the $HQ_{150}$ event. It can be seen, that without driftwood the deposition volume is controlled by the beam distance. The elongated basin results in less bedload deposition compared to the pear-shaped basin.

The experimental runs for the $HQ_{150}$ with bedload transport and added driftwood are shown in Figure 7. Compared to the experiments without driftwood slightly higher (on average) deposition volumes were recorded for the narrow beam distance of 10,5 mm. For the wider beam distance the deposition volumes are increased, but show a very high scatter. The high variability in the deposition behaviour can only be described by the chaotic and unpredictable clocking behaviour of the wood. The same effect was found in the pre investigation (TROJER 2013).

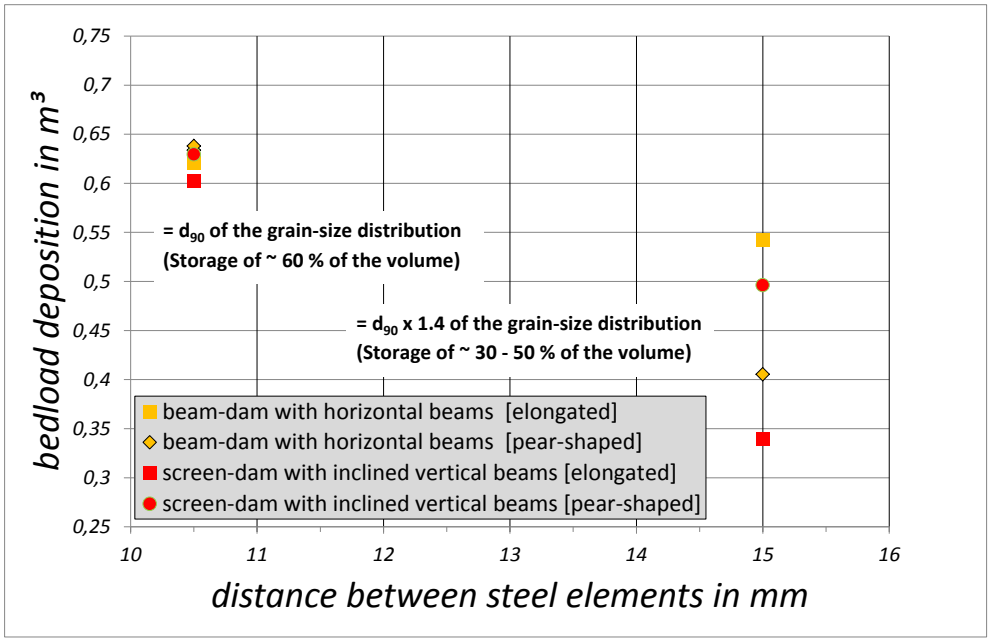


**Figure 6: Experiments with bedload without drift wood. The volumes are given for the deposition basin.**

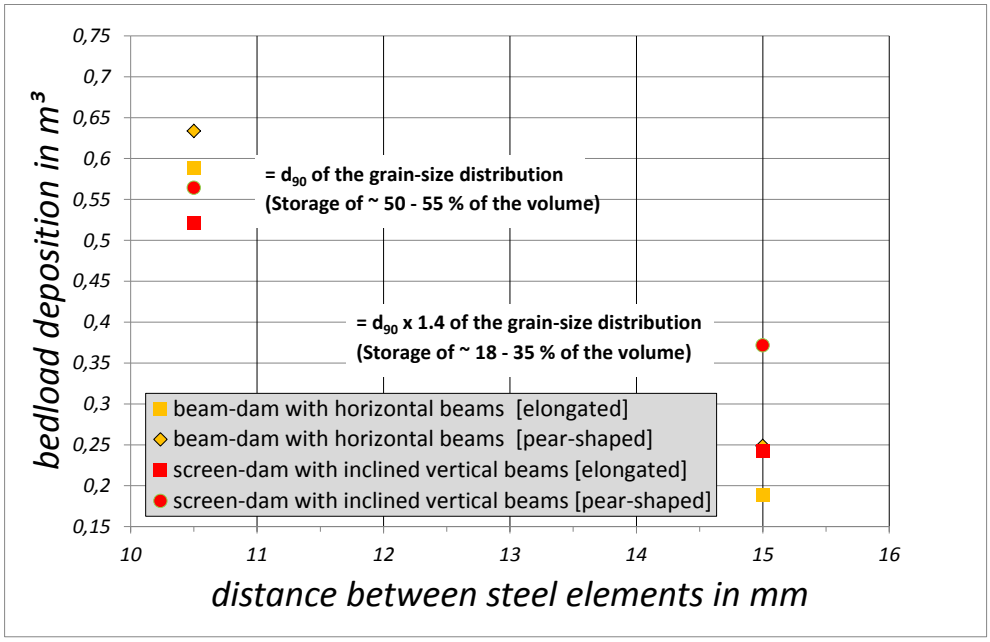


**Figure 7: Experiments with bedload and drift wood [Nr. 2,3,7,8,12,14,17,21]. The volumes are given for the deposition basin.**

The results have been further analysed concerning the possibility of self-emptying. Therefore the self-emptying efficiency has been calculated as described above and the rates are plotted against the beam distance. Figure 8 shows the results of the experiments without driftwood. Again, the beam distance controls the passing volume, but no effect of the shape of the deposition basin was found. The results for the experiments with additional driftwood are shown in Figure 9. It has to be reminded, that the driftwood has

been removed in-between the $HQ_{100}$ and $HQ_5$. The data with driftwood show a higher scatter. The efficiency of the experiments with the wider beam distance seems to be higher, but this can be attributed to the fact, that during the $HQ_{100}$ more sediment has been trapped.

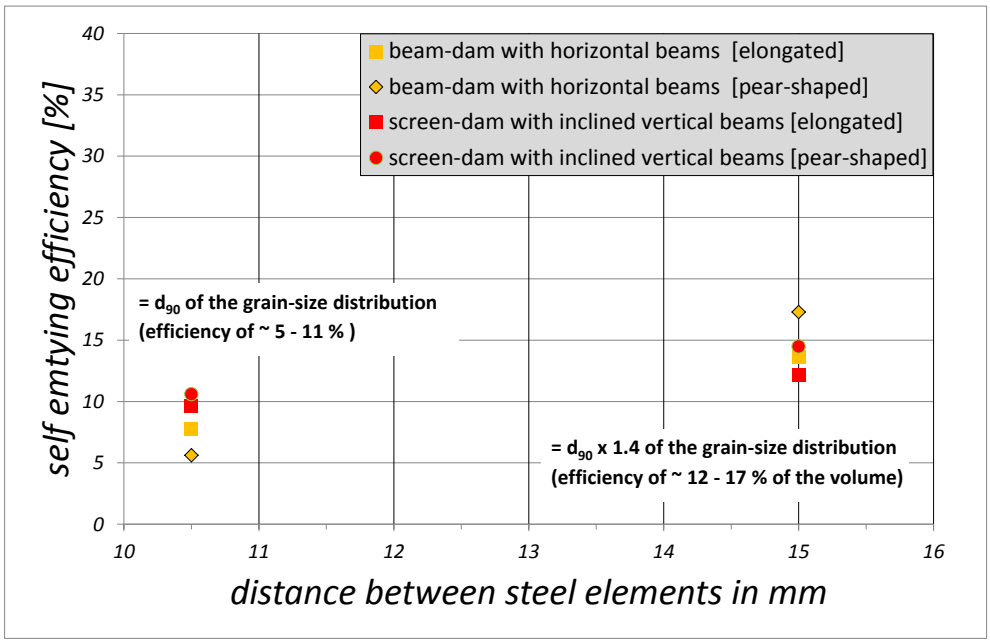


**Figure 8: Self-emptying efficiency for the experiments with bedload without drift wood.**

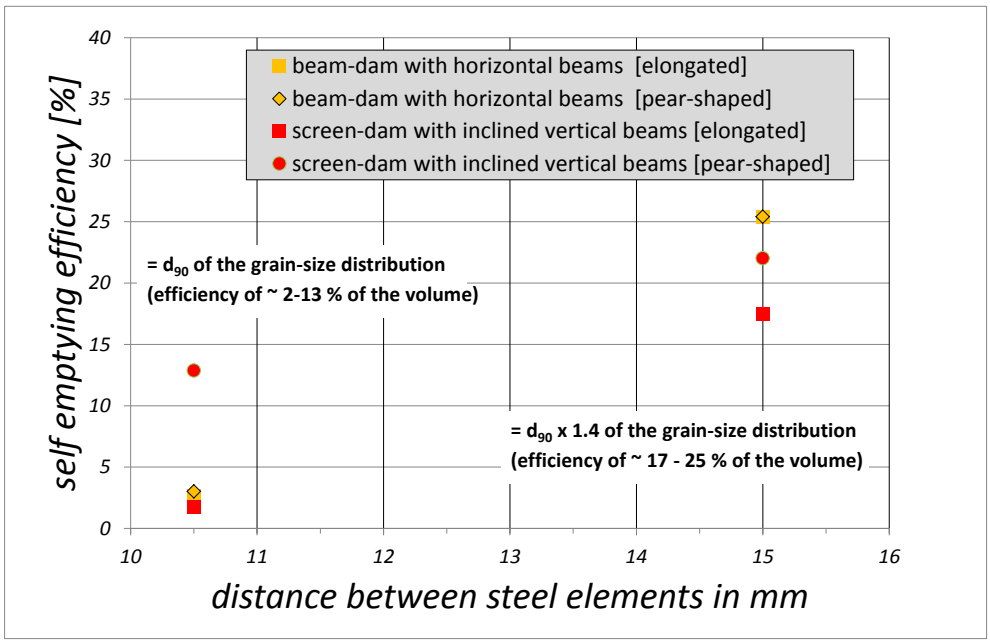


**Figure 9: Self-emptying efficiency for the experiments with bedload without drift wood.**

### 5.1.4 Grain sorting

Grain-size distributions were analysed in the deposition area and from the passing sediment. No grain sorting effect was found. In a statistical sense there has not been a

difference between the deposited and transported sediment. This can be explained by the function of the dams. Deposition did not start at the dam (no mechanical sorting due to the openings). All depositions started due to the reduced transport capacity at the inlet of the deposition area. Two effects play a major role: reduced transport energy due to the milder slope in the basin and widening which results in smaller flow depth.

### 5.1.5 Conclusions and Recommendations

The actual project and the pre-investigations showed that the deposition during the experiments was not controlled by sorting-effects at the location of the dam. The deposition always started from upstream, where the transport capacity was reduced due to the milder slope and the widening of the basin. No grain sorting effects could be identified. Finally it can be stated:

1. The deposition volume can be controlled by the beam distance if there is no driftwood.
2. The pear shaped basin resulted in higher deposition than the elongated basin.
3. Driftwood causes clocking of the dam and therefore higher deposition of bedload material.
4. Due to the chaotic behaviour of the log jams, driftwood causes a higher variability in the deposition behaviour.
5. Driftwood often causes log jams at the filter structure and therefore increases the trapping efficiency for bedload material. Beam dams with horizontal beams produce worse log jams than screen dams with inclined vertical beams. This effect is shown in Figure 10.
6. Even if the log-jams are removed, the self-emptying efficiency is limited. No statistically significant shape or filter structure type effect could be proofed.

**Figure 10: Different clocking behaviour of the dam types.**

## 5.2. Hydraulic scale model tests for the analysis of bedload transport processes in stepped torrent channels

Markus Moser - BMLFUW

Markus Aufleger, Bernhard Gems, Michael Sturm - UIBK

### 5.2.1 Problem setting and objectives

To determine the sediment input into receiving channels and, along with it, the risk of flooding and overbank sedimentation, the knowledge of bedload transport processes is necessary at the functional part of the barrier, as well as in the torrent channel (alluvial cone) to the receiving channel.

A project goal is to generally analyse and further optimize the bedload transport characteristics in the torrent channel to the recipient. Knowing the sediment inputs from the tributaries is very important for the protection of the lower reaches. For this purpose, the existing scale hydraulic model of the Schnannerbach (Tyrol, Austria) in the hydraulic laboratory at the University of Innsbruck was used to make further investigations. In the original tests, several experiments were carried out to increase sediment transport capacity of the Schnannerbach torrent channel and its confluence with receiving river Rosanna. On the actual state of the channel and on the optimized conditions, steady-state tests and as well a fully unsteady reconstruction of the 2005-flood event were performed. All tests were carried out under mobile bed conditions. Different grain size distributions, according with field survey data, were tested.

The aim of the experiments mainly is a qualitative assessment of the capacities in the torrent channel and the confluence zone and, further, the transport rates in the torrent channel in order to define critical sediment loadings and grain size mixtures, which lead to an overload of the torrent channel. Additional experiments within SedAlp project should investigate the influence of different gradient changes of the torrent channel in combination with different grain size distributions of the sediment input.

### 5.2.2 Planning approach - Model Setup and targets of the experiments

The Schnannerbach torrent in the Tyrolean Limestone Alps is an orografically left tributary of the Rosanna river in the Stanzertal. The torrent drains a 6.3 km² large catchment. The catchment is mainly exposed to the south. A gorge trail with a length of about 200 meters leads the Schnannerbach to a densely populated alluvial fan (district Schnann, municipality Pettneu am Arlberg).

The Schnannerbach represents a typical Alpine limestone mountain stream which is mainly dominated by fluvial sediment processes. Flood events with a relevant hazard potential for the populated alluvial fan are characterized by long-lasting precipitation events with moderate intensities, leading to medium and high discharges above the critical runoff and, correspondingly, fluvial bedload transport processes. According to the assessment of the "Wildbach- und Lawinenverbauung" the 150 years-design-flood is about 24m³/s. The expected amount of bedload, which is potentially mobilized under torrential hazard conditions, is thereby estimated to about 35.000 m³. With regard to the protection from harm-bringing flood events sediment retention barriers were built in the middle reach of the Schnannerbach. After emerging from the gorge trail, the torrent flows over the alluvial

fan in an approximately 12% steep sequence of steps and pools and finally leads into the Rosanna river.

Flood events in the recent past, in particular the event from August 2005, caused large damages in the settlement areas on the alluvial fan. The protection dams in the middle part of the reach could not hold back the entire sediment loads. Regressive aggradation processes in the torrent channel and aggradation processes in the Rosanna river at the confluence point led to massive water and sediment spills.

The main task of the Schnannerbach scale model experiments is the structural optimization of the river channels to fully prevent overbank flooding for the design case of a 150-annual event. Due to the improved data base, the design case was changed to the flood event from August 2005. The experimental programme is comprised of various structural measures in the Schnannerbach torrent channel and as well in the Rosanna river. The characteristics of the observed sediment grain sizes correspond to investigations made in the catchment area after the flood event in August 2005. Further, after the reconstruction of the 2005 flood event and with it the validation of the scale model and the definition of critical loading conditions, numerous experiments were simulated under steady-state discharges. They were aimed to determine effects of different optimization options and to determine the resulting transport capacities in the river channels.

The model was built at a scale of 1:30, it conforms to Froude similarity. It covers about 280 m of the Schnannerbach torrent to the confluence with the Rosanna river. The latter is covered over a length of 200 m. The model boundaries are shown in Figure . An overview of the scale model in its original condition is illustrated in Figure 1.

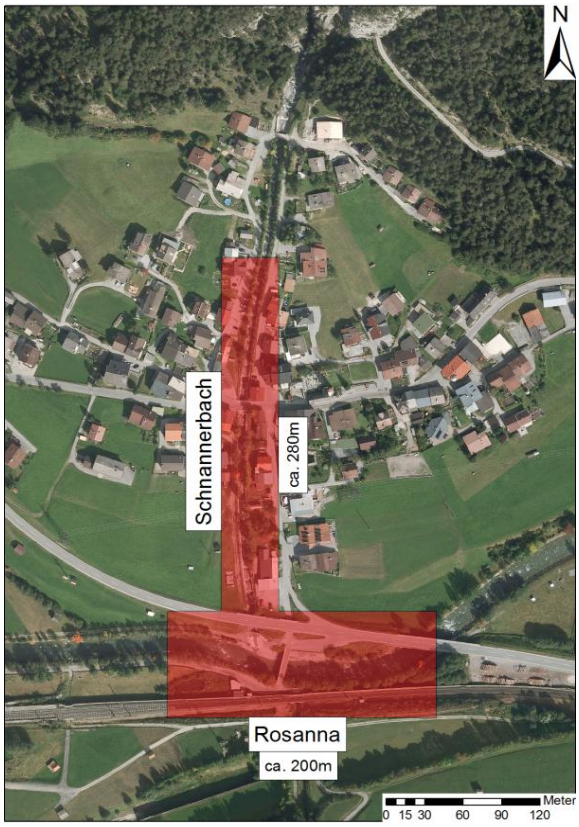


**Figure 1: Extent of the hydraulic scale model of the Schnannerbach torrent and the Rosanna river (1:30)**

**Figure 2: Hydraulic scale model in its original condition at a scale of 1:30**

Based on the experiments for generally improving flood protection at the alluvial fan of the Schnannerbach torrent, further experiments were executed to examine the sediment transport of the torrent channel without the influence of the receiving water course. The essential factors in this case, the torrent channel gradient and the impacting bedload characteristics, were analysed. In these experiments, the draining channel was completely removed in order to prevent regressive aggradation and backwater effects.

### 5.2.3 Construction of the model, methodology and test arrangement

To investigate the influence of the torrent channel gradient, an artificial decrease in the channel was built which is intended to simulate a flatter slope and thus lower transport rates.

Three different gradient changes were tested: The first gradient change was from the original approximately 12 % gradient to a 9 % gradient, the second from 12 % to 7.5 % and the third from 12 % to 6 %.

For every of these situations, steady-state experiments with three different grain size distributions for the sediment input were simulated. The grain size distributions were taken from the event documentation of the flood event 2005 (Rudolf-Miklau et al., 2006) and were adjusted for the model tests. With regard to unrequested scale effects the smallest grain size is limited to 0.5 mm for the experimental modelling. The mean grain size distribution corresponds to the original Schnannerbach model tests and matches with the average grain size distribution of the four measurements taken from the Schnannerbach after August 2005. For the finer and coarser grain mixtures, the measurements from other streams with local reference to the catchment area of the Schnannerbach were taken. The upper and the lower limits of these grain size distributions correspond to the coarser and finer sediment mixtures. The different grain size distributions are shown in Figure 11.

All experiments were carried out under steady-state conditions with a duration of about 82 minutes each (prototype dimensions). The sediment loads are equal for every simulation and correspond to a fraction of about 12 % of the water discharge. For fluvial processes this fraction represents the measured critical transport capacity of the channel section with a gradient of app. 12 %.

The discharge for the steady-state experiments (17.8 m³/s) is similar to the mean flow of the rising flood wave from August 2005 (Chiari, 2008) and was classified as the most critical load case in combination with this sediment fraction (Sturm et al., 2014). Further discharges were tested on the middle bend situation (change in gradient from 12 % to 7.5 %). A larger (26.8 m³/s) and lower discharge (8.8 m³/s) were performed, again with a constant sediment fraction of 12 % each.

All experiments were documented with photographs and videos. To create a mass balance study of the transported sediment loads, the sediment output of the tests was dried and weighted for every experiment.

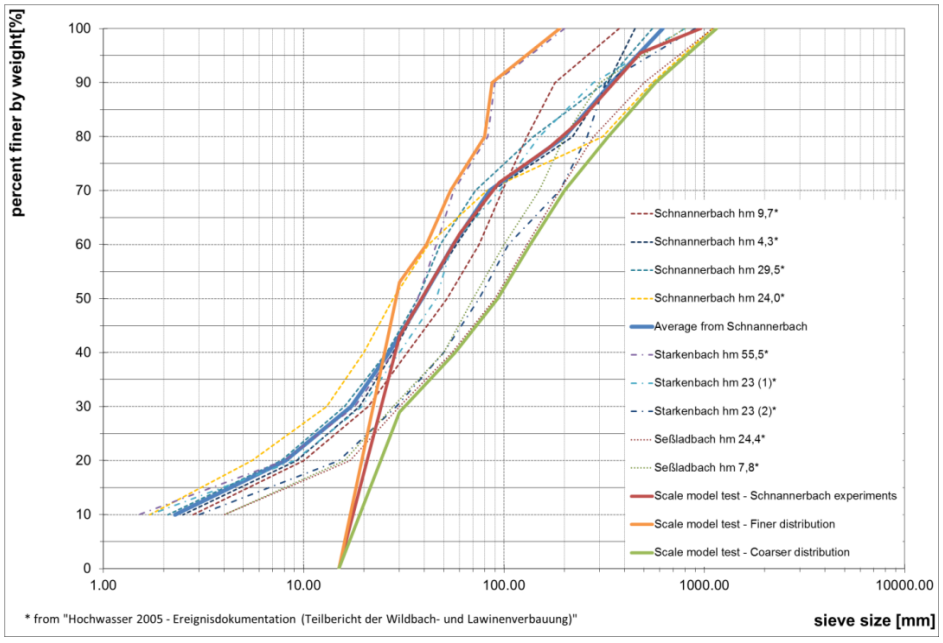


**Figure 3: Characteristic grain size distributions of the Schnannerbach catchment and neighbouring torrent catchments; grain size distributions for the hydraulic scale model tests (prototype dimensions)**

### 5.2.4 Results, Conclusions and Recommendations

The original experiments considering the Schnannerbach torrent channel and the confluence with the Rosanna river clearly showed that the optimization in the receiving water is not sufficient enough to transport all incoming from the tributary sediment. Consequently, bedload management has to be improved also at the retention structures in the upper catchment of the Schnannerbach torrent.

However, the transported sediment can be significantly improved with a few structural optimizations on the alluvial fan. Overbank flooding and sedimentation during a flood event according to the event from August 2005 can be delayed significantly and the

damages on the alluvial cone can be minimized with it. The following optimizations in the confluence zone were found to be the best:

1. Heightening of the sidewalls of the Schnannerbach torrent channel in the near range of the confluence point
2. Extension of the sidewalls of the Schnannerbach torrent to the confluence point
3. Optimization (lowering) of the intersection-angle
4. Lowering of the Schnannerbach mouth to increase the gradient in the last section of the Schnannerbach torrent

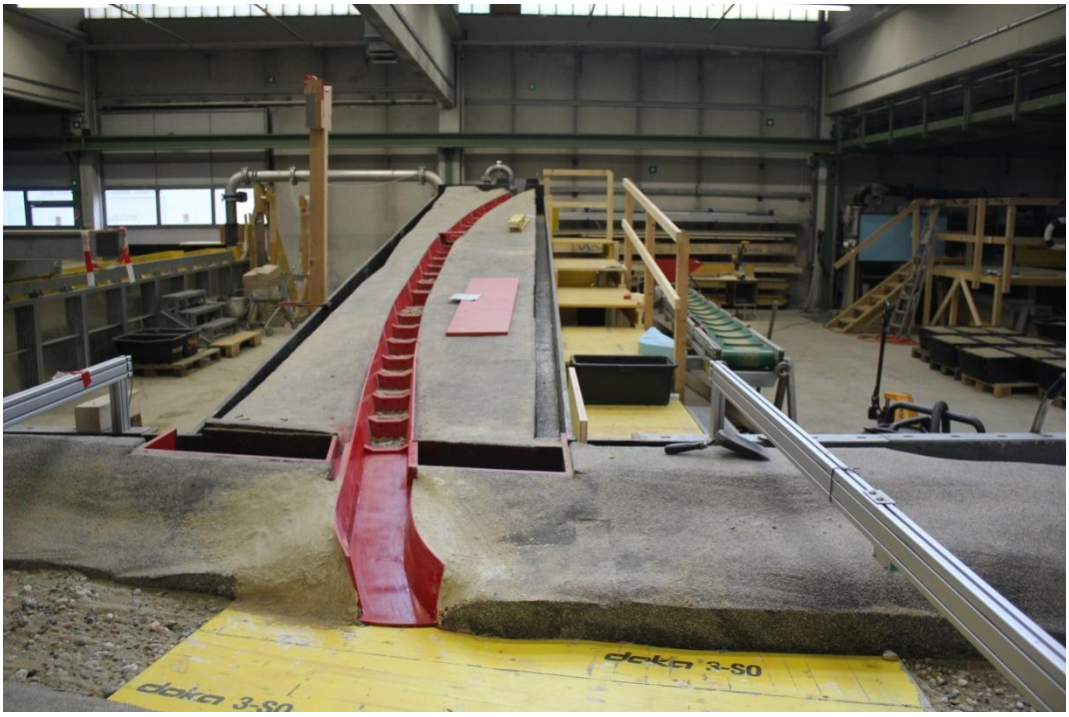


**Figure 4: Schnannerbach torrent and Rosanna river featuring the final optimization measures**

Further investigations showed, that massive structural optimizations at the confluence in the Rosanna river yielded only very small improvements with explicit enhancement of the water-level of the Rosanna. A flat river bed of the torrent channel without steps and pools provided a better transport capacity of the Schnannerbach, but not on the entire system, in which the deposits at the confluence are significant.

In general it was established that the transport in the torrent channel is significantly influenced from the conditions in the confluence area. The Schnannerbach torrent channel in its original condition may cope with a sediment fraction of about 12%. The entire system with the confluence zone can dissipate a sediment fraction until 6 % until overbank sedimentation appears firstly just upstream the state road bridge. In order to achieve a clogging of the village bridge a sediment fraction of 12 % is further necessary. For this reason, these two critical spots along the torrent channel can be defined. On the one hand, the state road bridge in which in all experiments, as well as in historic flood events, the overbank sedimentation firstly appears. The second spot is represented by the village bridge. All these findings are based on the simulation of the 2005-flood event characteristics.

An interesting process behaviour related to the bedload transport in the stepped torrent channel is surging. Originally suspected as a model scale effect due to an inaccurate sediment supply at the Schnannerbach model boundary, this effect can mainly be related to the hydraulics and the transport process through the steps and pools of the torrent channel. A distinctive surge pattern could be observed as early as the sediment fraction increased about 1.6 %. However a corresponding river bed shape is necessary. With increasing sediment input the steps and pools disappear and a flat river bed develops. On this flat river bed there was no surge observed. A positive aspect of these surges is that it forces the onward movement of bedload in the confluence zone.

The additional experiments within the SedAlp-project showed the influence of different gradient changes and different grain size distributions on the sediment transport rates in the torrent channel. With a gradient change from 12 % to 9 % no overbank occurred in all simulations. A further reduction of the channel gradient to 7.5 % leads to flooding, when testing with the two coarser grain size distributions. The experiments with a gradient change from 12 % to 6 % led to overbank sedimentation with all tested grain size distributions. There could be also a difference in the way of overbanking observed: While with coarse grain size distributions the flooding appears rapidly, this process is a bit sluggish with finer grain sizes. The overload of the channel occurs in all cases pretty much at the spot where the gradient changes. Starting from this point, similar to the original Schnannerbach experiments, regressive aggradation occurs towards the village bridge further upstream.

Figure 5 shows a snapshot the scale model during an experiment for the SedAlp project. The red line marks the gradient change and the spot of the first overbanking. The picture was taken during the experiment with a gradient change from 12 % to 6 % and the coarser sediment mixture.

**Figure 5: Steady-state conditions in the Schnannerbach torrent channel; situation with a change in gradient from 12 % to 6 % at the red line – conditions after 16 minutes (prototype dimensions) of modelling**

## 5.3 Physical model report

Sindelar Christine, Schobesberger Johannes, Mattersberger Elisabeth, Eichinger Georg and Helmut Habersack - BOKU

### 5.3.1 Introduction

In recent years the doctrine of flushing the reservoir of a run-of river hydropower plant (HPP) as rarely as possible to prevent negative ecological impacts has changed. Today, the concept of flushing the reservoir frequently is widely accepted and was an important outcome of the INTERREG IIB project ALPRESERV (eg. Schneider et al. 2007; Badura et al. 2007). Flushing a reservoir frequently improves the longitudinal sediment continuity in rivers. Moreover, the turbidity rates of a particular flushing event are reduced, thus minimizing fish mortality.

In the present experimental case study we aimed to investigate the effect of different structural measures of a run-of river hydropower plant (HPP) on the flushing capabilities.

### 5.3.2 Experimental setup

A physical model test of a low head run-of river HPP was conducted at the Hydraulics Laboratory of the University of Natural Resources and Life Sciences in Vienna, Austria. The physical model doesn't correspond to a particular prototype river. It represents an idealized middle-size gravel bed river having a width of 20 m, a slope of 0.0065 and a mean annual flow of 15 $m^3/s$. The 1-year flood is 80 $m^3/s$. The gravel has a characteristic grain size $d_{90}$ of 62 mm. The model scale is 1:20. The physical model is 15 m long. It consists of a straight head water section and the reservoir of the HPP. The HPP is simply modelled by three or four fields of equal width separated by weir piers. The number of fields depends on the investigated scenario (Figure 1, Figure 3). Each field can be opened and closed by means of a sluice gate. Each field can either represent the turbine inlet which is closed during the flushing operation or a weir field which is open during the flushing operation.

It is well known that the sedimentological time scale in scaled mobile bed experiments can be determined only if field data is available to calibrate the model (Kobus, 1984). As we are dealing with an idealized river no such filed data is available. We therefore assume that the sedimentological time scale $L_{t,s}$ is identical to the hydrodynamic time scale in a Froude model, thus $L_{t,s}=20^{1/2}$.

We postulate undisturbed sediment transport from the upstream river reach. The sediment transport rate for different discharges was determined in preliminary tests. The sediment transport formula from Smart and Jäggy (1984) was adjusted accordingly to yield reliable results within a range of flood events of short return periods.The postulated prototype and experimental conditions are summarized in Table 1.

**Table 1: Prototype and experimental conditions**

| | **Prototype** | **Scaled model** |
|---|---|---|
| Mean annual flow $Q_M$ | 15 $m^3/s$ | 8.4 l/s |
| 1-year flood $Q_1$ | 80 $m^3/s$ | 44.7 l/s |
| river width b | 20 m | 1 m |
| Slope of upstream river width $S_r$ | 0.0065 | 0.0065 |
| Characteristic grain diameter $d_{90}$ | 62 mm | 3.1 mm |
| Sediment transport rate $q_s$ for $Q_1$ | 2.1 kg/sm | 23.6 g/sm |

### 5.3.3 Structural measures

The following structural measures were investigated.

**S1** height of the weir sill (this has an effect on the mean bed slope S in the reservoir)

**S2** widening of river width towards the weir system

**S3** location of the turbine inlet: in extension of the straight left bank / in extension of the widened right bank

**S4** height of the guiding wall to divert sediments away from the turbine inlet

We further varied the degree of siltation

- the reservoir is empty, the bed slope in the reservoir is S
- the reservoir is siltated by 0.6 meters at the weir system. The siltation extends horizontally upstream until it intersects with the upstream river bed

### 5.3.4 Experimental procedure

For a fixed set of structural measures a test series was conducted. It consisted of several test runs. Prior to a test series a plane bed of slope S was adjusted. By means of photogrammetry the initial bed levels were determined at a spatial and vertical resolution of less than a millimeter. Then the desired discharge was adjusted. Sediments were fed to the model automatically and continuously at the beginning of the test section. During a test run of a 1-hour period the water and bed levels were recorded several times by means of a point gauge. The entrained sediments were collected in a sand trap at the downstream end of the model. After the test run the bed levels were again captured by means of photogrammetry. A test run was repeated until equilibrium conditions were reached, i.e. the fed sediment mass equaled the sediment output in the sand trap.

### 5.3.5 Postprocessing

The sediment balance (input – output) was determined from two different procedures: (i) the fed sediment input mass is known. The sediment output is determined by weighing the

sediments in the sand trap box (ii) from the photogrammetric surveys digital elevation models (DEM) are generated. By subtracting the two digital elevations models (DEM) before and after a test run the volume can be determined. Multiplying the volume with the bulk density of the model sediments yields the resulting mass.

### 5.3.6 Scenarios and their flushing capabilities

For the 1-year flood the structural measures S3 and S4 do not have a significant effect on the flushing capabilities. For the design recommendation four different scenarios were analyzed and interpreted (Table 2).

**Table 1: Investigated scenarios and their flushing capabilities**

| | slope | widening | B/b | siltation |
|---|---|---|---|---|
| Scenario 1 | 0.0065 | yes | 4/3 | no |
| Scenario 2 | 0.0065 | no | 1 | no |
| Scenario 3 | 0.0030 | no | 1 | no |
| Scenario 4 | 0.0065 | no | 1 | yes |

#### 5.3.6.1 Scenario 1

In scenario 1 the slope in the reservoir is 0.0065 which is equal to the assumed slope $S_r$ of the upstream river reach. The weir system of scenario 1 consists of four fields; the one on the left bank represents the turbine inlet. During the flushing operation (i.e. during the experiment) the turbine inlet is closed. Upstream of the turbine inlet a guiding wall is arranged to divert sediments away from the inlet. The remaining three fields represent the weir fields which are open during the flushing operation. On the right bank the river is widening towards the weir system. The widening ratio is 4/3 (Figure 1). It is very common to extend the river width at the HPP such that the weir system (without the turbine inlet) covers the whole river width. This way it is easier to guarantee that high flood events can be conveyed over the weir system even in the case of failure of one of the weir gates.

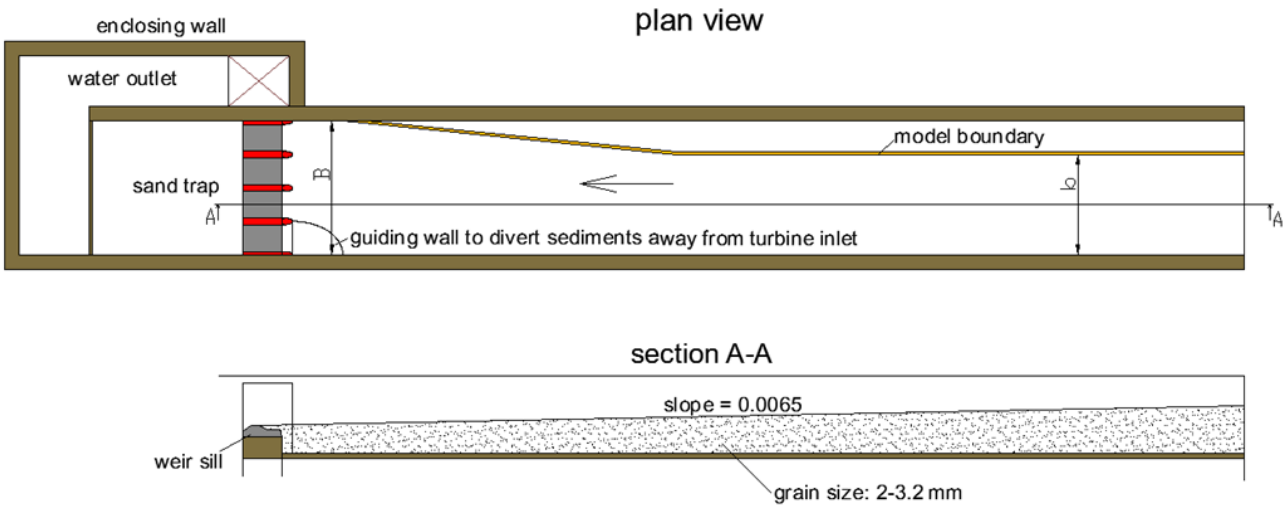


**Figure 1: Scenario 1 – widening B/b = 4/3, slope S=0.0065, without siltation, guiding wall in front of the turbine inlet**

In Figure 2 the normalized sediment addition and output are plotted for each test run of scenario 1. For normalization the added mass is divided by the set sediment addition, the mass output is divided by the actual sediment addition. A value of 1.0 for the sediment addition thus means that the actual sediment addition coincides with the set sediment addition. A value of 1.0 for the normalized sediment output means that actual sediment addition and sediment output are equal. Dynamic equilibrium is reached after 6 test runs, i.e. after 6 hours which corresponds to duration of approx. 27 hours at prototype scale.

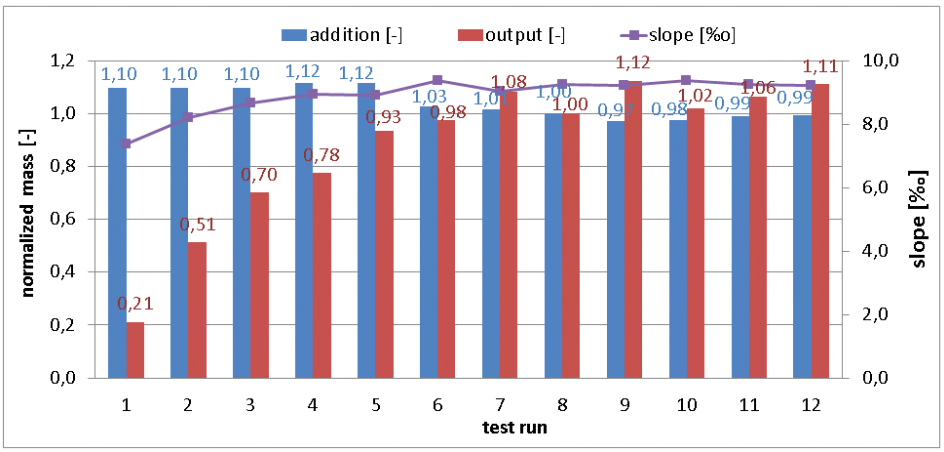


**Figure 2: Normalized sediment addition, normalized output and mean bed slope in the reservoir for each test run of scenario 1**

### 5.3.6.2 Scenario 2

In scenario 2 the slope in the reservoir is 0.0065 which is equal to the assumed slope of the upstream river reach. The weir system of scenario 2 consists of three fields, all of them representing weir fields which are open during flushing operation. The reservoir is a straight channel without widening. It is assumed that there is a diversion tunnel in the reservoir to the power house of the HPP which is omitted in the physical model (Figure 3).

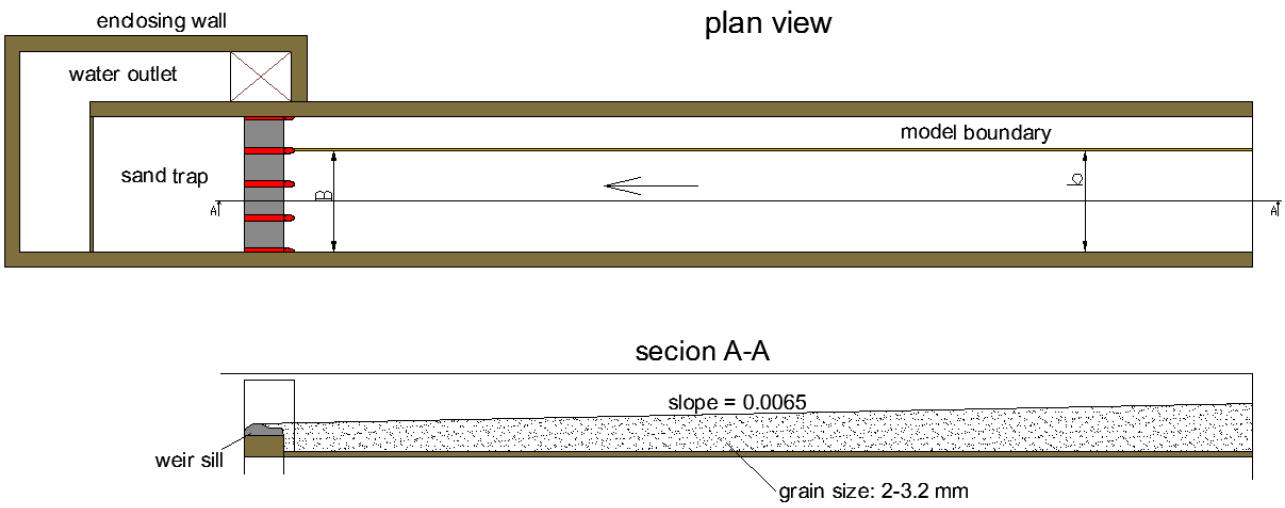


**Figure 3: Scenario 2 – without widening, slope S=0.0065, without siltation, three weir fields, turbine diversion tunnel not modeled**

In Figure 4 the normalized sediment addition and the normalized output are plotted for each test run of scenario 2. Dynamic equilibrium is reached after 3 test runs which corresponds to duration of approx. 13 hours at prototype scale.

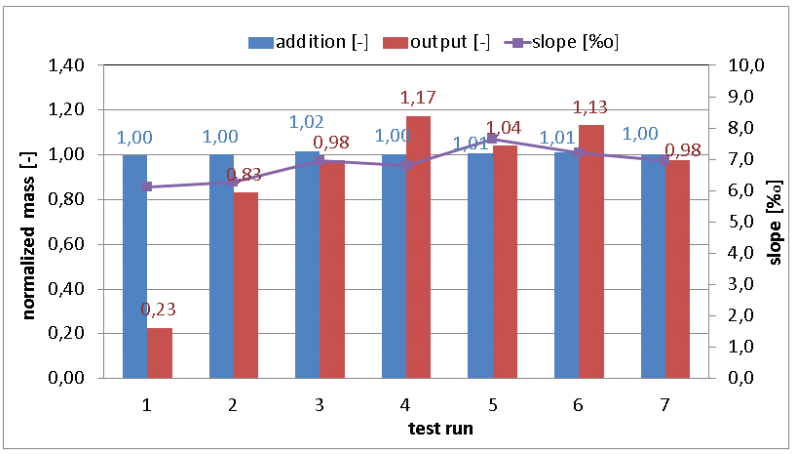


**Figure 4: Normalized sediment addition, normalized output and mean bed slope in the reservoir for each test run of scenario 2**

### 5.3.6.3 Scenario 3

In scenario 3 the slope in the reservoir is 0.003 which is less than half of the assumed slope of the upstream river reach. The flat slope in the reservoir is a result of the heightened weir sill. Typically the weir sill is higher than the original river bed level to save construction costs. The weir system of scenario 3 consists of three fields, all of them representing weir fields which are open during flushing operation. The reservoir is a straight channel without widening. It is assumed that there is a diversion tunnel in the reservoir to the power house of the HPP which is omitted in the physical model (Figure 5).

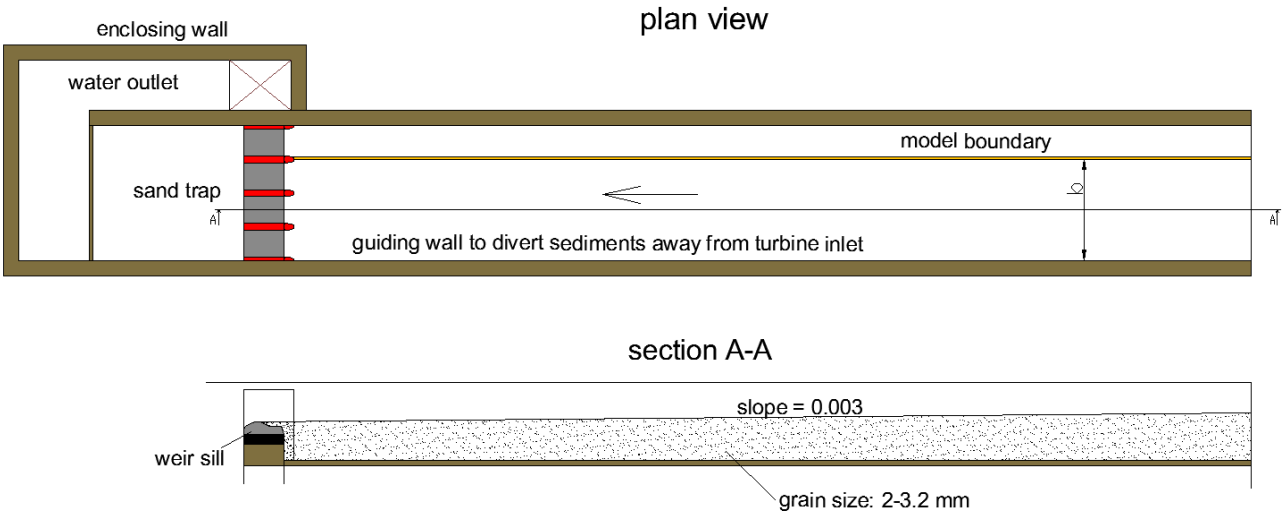


**Figure 5: Scenario 3 – without widening B/b = 1, slope S=0.003, without siltation, three weir fields, turbine diversion tunnel not modeled**

In Figure 6 the normalized sediment addition and the normalized output are plotted for each test run of scenario 3. Dynamic equilibrium is reached after 7 test runs which corresponds to a duration of approx. 31.3 hours at prototype scale.

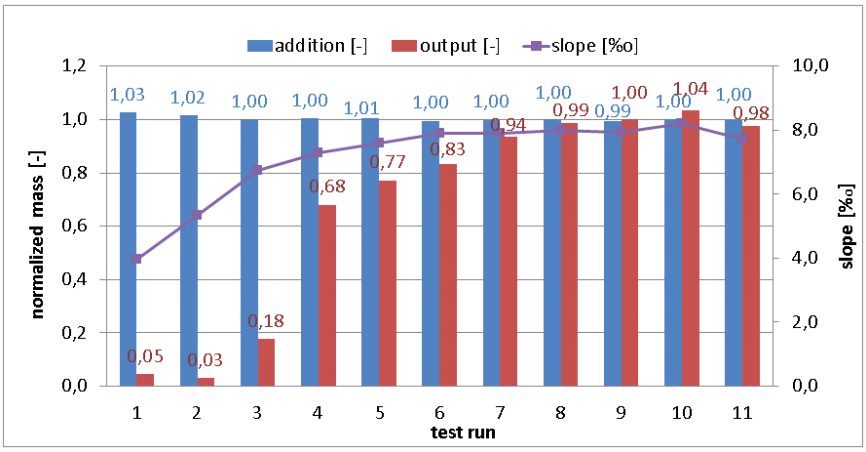


**Figure 6: Normalized sediment addition, normalized output and mean bed slope in the reservoir for each test run of scenario 3**

### 5.3.6.4 Scenario 4

In scenario 4 the slope in the reservoir is 0.0065 which is equal to the assumed slope of the upstream river reach. The weir system of scenario 4 consists of three fields, all of them representing weir fields which are open during flushing operation. The reservoir is a straight channel without widening. It is assumed that there is a diversion tunnel in the reservoir to the power house of the HPP which is omitted in the physical model. The degree of siltation is 0.6 m at the weir system (Figure 7).

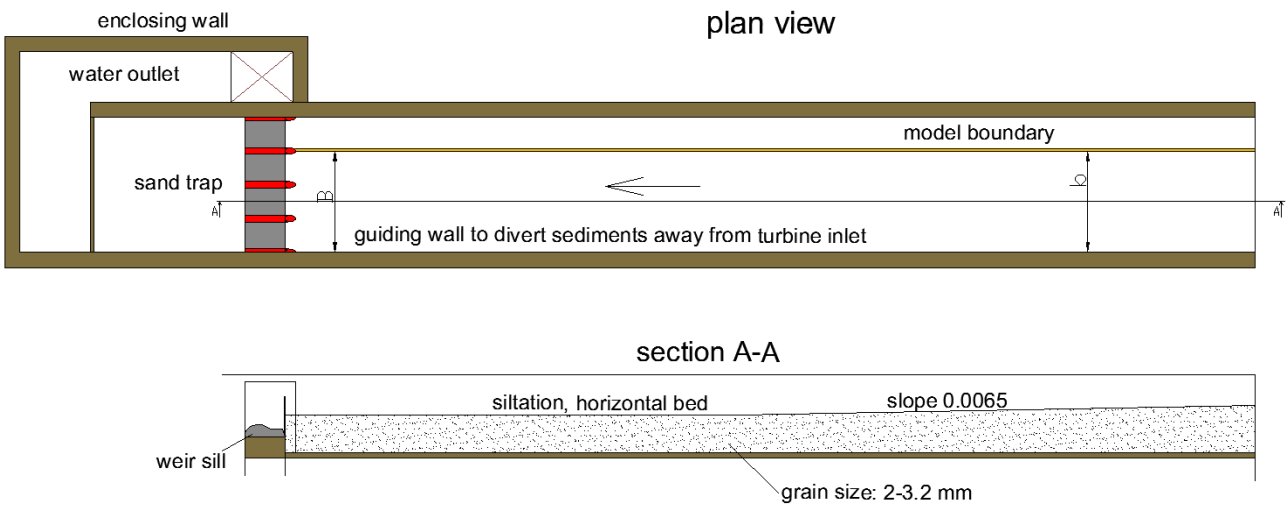


**Figure 7: Scenario 4 – without widening B/b = 1, slope S=0.0065, degree of siltation: 0.6 m at the weir system, three weir fields, turbine diversion tunnel not modeled**

In Figure 8 the normalized sediment addition, the normalized output and the normalized siltation are plotted for each test run of scenario 4. For normalization, the degree of siltation (kg) is divided by the initial degree of siltation (kg). A value of 0.5 for the normalized siltation means that the initial siltation has been cut in half. In each test run more than the added sediments are entrained. As a result the degree of siltation in the reservoir is reduced. In test run 1 the reduction of siltation is especially pronounced. This is not surprising as the initial bed level is higher than the weir sill level. Therefore the sediments in the vicinity of the weir sill are entrained immediately after the gates are opened.

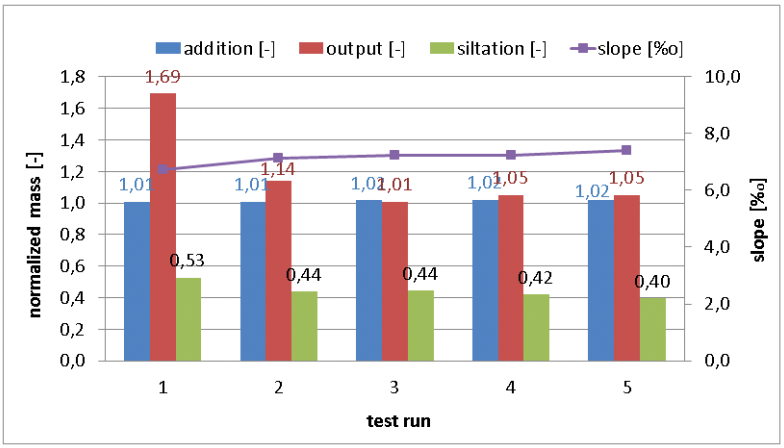


**Figure 8: Normalized sediment addition, normalized output, normalized siltation and mean bed slope in the reservoir for each test run of scenario 4**

### 5.3.7 Limitations – simplifications

The conducted experimental study is the first basic experiment of its kind aiming at finding design recommendations for run-of river HPPs with the focus on enhanced flushing capabilities. The experimental setup is simple and subject to certain limitations. The experiments were run

- with sediments having a uniform grain size distribution, $\sigma=(d_{84}/d_{16})^{1/2}=1.17$

- without small grain size fractions
- without cohesive sediments
- under steady conditions
- Typically, the turbine inlet is located upstream of the weir gates. Due to the simple modular construction of the physical model, the turbine inlet is aligned laterally with the weir gates.
- for the non-widened reservoir a solution has to be developed for a diversion turbine tunnel

### 5.3.8 Results and design recommendations

In order to interpret the experimental results we have to define a criterion to determine if the flushing operation was successful. We call a flushing event "successful" if the degree of siltation in the reservoir is less after the flushing than before the flushing. This criterion is purely hydro-morphodynamic. It does not take into account ecological implications of the flushing event. In Table 2 the minimum flushing duration [h] at prototype scale is given to ensure successful flushing for a 1-year flood event. The initial and the equilibrium bed slope of the reservoir are also listed.

**Table 2: minimum flushing duration at prototype scale to ensure "successful flushing"**

| | Initial slope | widening | B/b | siltation | Equilibrium slope | flushing duration [h] |
|---|---|---|---|---|---|---|
| Scenario 1 | 0.0065 | yes | 4/3 | no | 0.0093 | 27 |
| Scenario 2 | 0.0065 | no | 1 | no | 0.0070 | 13 |
| Scenario 3 | 0.0030 | no | 1 | no | 0.0079 | 31 |
| Scenario 4 | 0.0065 | no | 1 | yes | 0.0073 | immediately |

As can be seen from Table 3 all scenarios yield a higher equilibrium slope than the initial slope. Scenario 1 corresponds to a common configuration of a HPP (Figure 1): The reservoir widens towards the weir system. Three weir fields cover the original river width b. The turbine inlet is located in the widening section. The ratio of widened river width B to the original river width b is 4/3 (Figure 9)

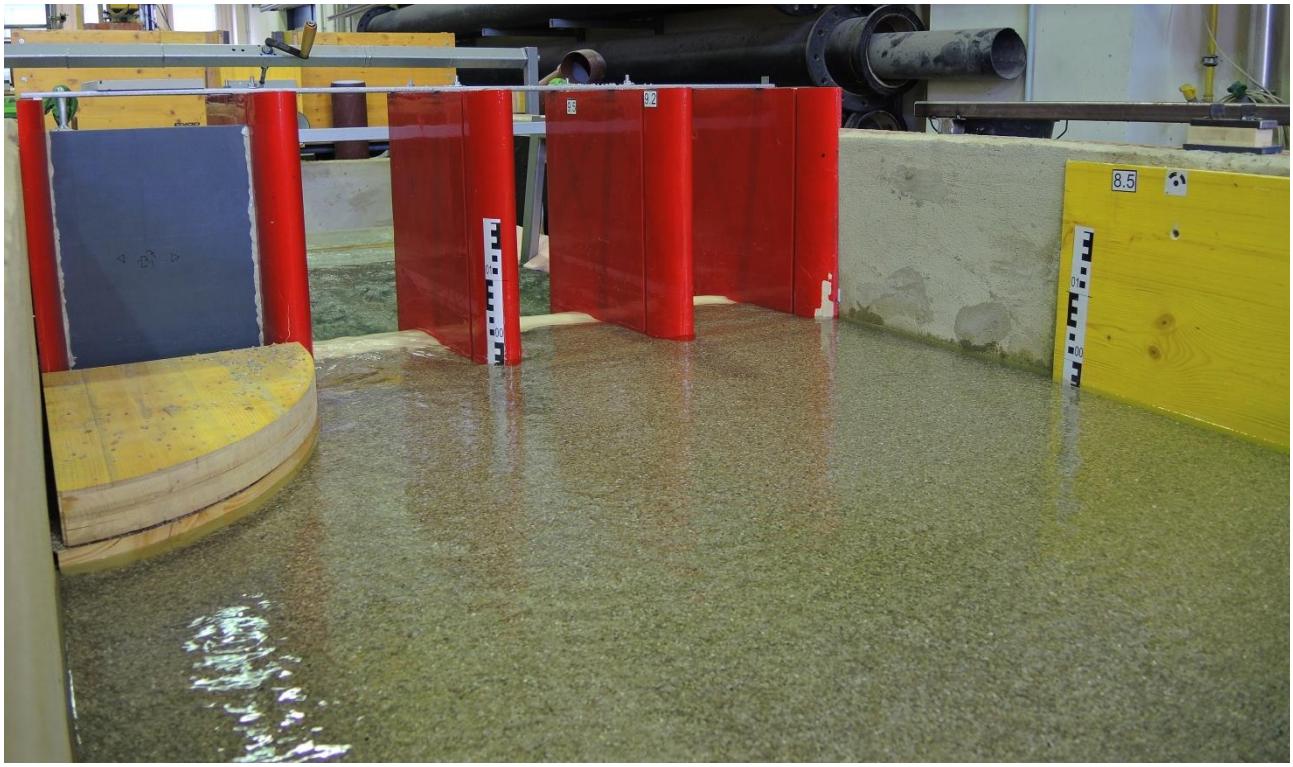


**Figure 9 physical model of scenario 1: closed turbine inlet with sediment guiding wall (left), three open weir fields (right)**

However, scenario 1 represents an ideal case since the weir sill is at a very low level such that the slope of the reservoir is equal to the slope of the undisturbed upstream river reach. Typically, the weir sill is set at a higher level to save building and material costs. The drawback is that the slope in the reservoir decreases. Scenario 1 is thus better suited to enhance sediment entrainment during flushing compared to a standard configuration with a reduced slope in the reservoir. For scenario 1, the initial bed slope increases from 0.0065 to 0.0093. It takes 27 hours to reach equilibrium conditions. Scenario 2 differs from a straight river reach only by the weir piers which reduce the cross section (Figure 3). This extra resistance increases the initial slope from 0.0065 to 0.007 at equilibrium conditions which are reached after 13 hours. Scenario 3 on the other hand is more realistic regarding the reduced slope in the reservoir (0.003) compared to the slope of the upstream river reach (0.0065). It takes 31 hours to reach equilibrium conditions and the equilibrium slope is 0.0079. In scenario 4 a silted reservoir is assumed (Figure 7). The initial mean bed slope in the reservoir calculated from the siltation level (rather than from the weir sill) is 0.0034 and is thus comparable to the configuration of scenario 3. However, the low weir sill demonstrates its effect immediately after the flushing starts. The deposited sediments close to the weir are entrained quickly.

To summarize, scenarios 1 and 3 perform similarly well regarding the minimum required time to guarantee a successful flushing. However, the slope required to reach equilibrium conditions is much higher for scenario 1 than for scenario 3. Typically, the peak flow for a 1-year flood is no longer than 24 hours. For scenarios 1 and 3 the minimum flushing duration is 27 hours. Thus, flushing operations for these scenarios will most likely be unsuccessful for a 1-year flood. Even worse, the standard configuration of a HPP typically corresponds to a combination of scenario 1 and 3, i.e. a widened area at the weir system and a heightened weir sill. The minimum required time to guarantee successful flushing will most probably increase significantly if both scenarios 1 and 3 are combined. The

minimum flushing duration of scenario 2 is only half as long as for scenarios 1 and 3. Scenarios 2 and 4 are identical except for the degree of siltation. The experiments of scenario 4 suggest that moderate degrees of siltation are harmless provided that the weir sill is sufficiently low.

From the experimental results two conclusions may be drawn:

1. The height of the weir sill has a huge effect on the flushing capabilities. With this respect it is recommended to design the weir sill such that the original slope of the upstream river reach is kept. The drawback is that the construction costs of a HPP will increase because higher gates and larger concrete works are necessary. On the other hand maintenance and operational costs will decrease because of the enhanced flushing capabilities.
2. The river widening towards the weir system which is typically found at run-of river HPPs significantly reduces the flushing capabilities. The equilibrium slope is significantly higher than for the non-widened scenarios. It is recommended to find new ways to keep the river width in the reservoir and to design a turbine diversion tunnel instead.

### 5.3.9 References

Badura, H., Knoblauch, H., Schneider, J., Harreiter, H., Demel, S. (2007): Wasserwirtschaftliche Optimierung der Stauraumspülungen an der Oberen Mur – Best practise flushing strategy at the Upper Mur River, Österreichische Wasserwirtschaft, Heft 5-6(59), p.61-68.

Eichinger, G. (2014): Konstruktive Gestaltung von Flusskraftwerken unter dem Aspekt der Stauraumentlandung. Master thesis, Institute of Water Management, Hydrology and Hydraulic Engineering, University of Natural Resources Vienna.

Kobus, H.: Wasserbauliches Versuchswesen. Deutscher Verband für Wasserwirtschaft und Kulturbau e.V. (DVWK) (Eds.), 2nd edition, Parey Verlag Berlin.

Mattersberger, E. (2014): Physikalischer Modellversuch zur Ermittlung des Gleichgewichtsgefälles. Master thesis, Institute of Water Management, Hydrology and Hydraulic Engineering, University of Natural Resources Vienna.

Schneider, J., Badura, H., Knoblauch, H., Frei, R., Eberstaller, J. (2007): Flushing of the run-of river plant Bodendorf in Styria/Austria in respect of technical an ecological impacts Proceedings of the 7th Int. Conf. on Hydroscience and Engineering (ICHE-2006), Sep 10 –Sep 13,Philadelphia,USA.

## 5.4 Test bed description – UNI PD Italy

Lorenzo Picco - TESAF

### 5.4.1 Chiesa stream

The Rio Chiesa is located into the Italian Alps, in the north-eastern part of Italy. Its basin is located in the municipality of Livinallongo del Col di Lana ( BL) ( 1.17 km2, 0.95 km2 at Livinallongo cross section).

The basin is characterized by a average elevation of about 1780 m.a.s.l., with a maximum and minimum elevation of about 1175 and 2462 m.a.s.l., respectively. The entire catchment present a mean gradient of about 75% and the mean stream channel gradient is around 45%, and the length of the main stream is about 1.75 km. This area is characterized by a mean annual rainfall of about 1200 mm.

The basin is characterized in its geology setting by the presence of Quaternary moraine, Wengen volcanic sediment, Werfen and the typical Livinallongo formation.

Land use is divided in thick woodland for about 65%, unproductive land for about21% and Shrubs for around 7% of the area.

The Rio Chiesa basin is regularly affected by events of debris flows that endanger the towns (especially Pieve di Livinallongo) and some important roads, creating dangerous conditions for the residents and the many tourists. Typically the hazard phenomena in the basin are debris flows or mud flows that start in the upper part of the basin in a range of altitude from 1900 m to 2100 m a.s.l. in an area subjected to erosion.

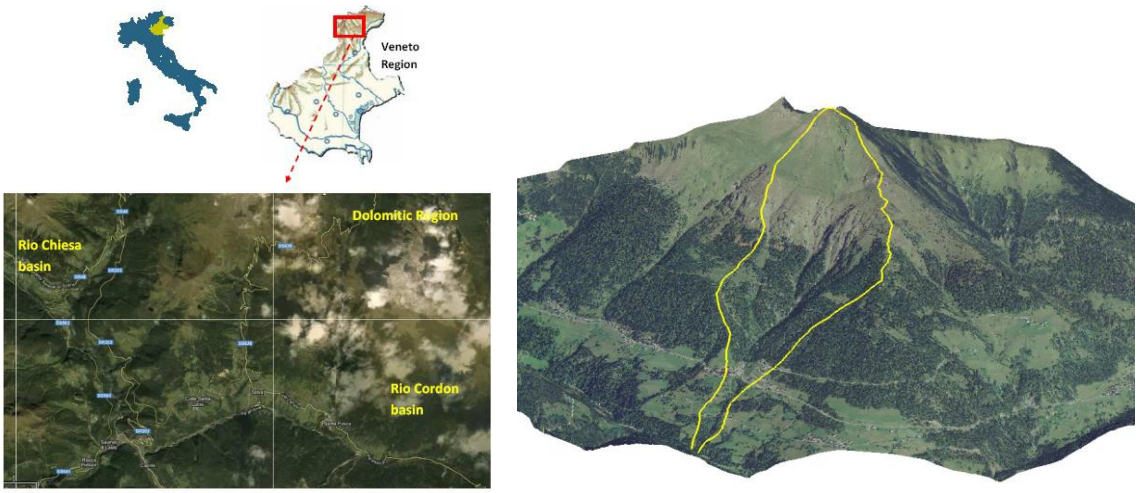


**Figure 1: Rio Chiesa basin localization (on the left), and basin delimitation( yellow line, on the right).**

### 5.4.2 Rio Rudan

#### 5.4.2.1 Testbed description

The Rio Rudan watershed is a small basin located in the Province of Belluno (Veneto Region) in the north-east Italy. It is characterized by an area of about 3003 km$^2$, an

average elevation of about 1689 m.a.s.l, with a minimum and maximum elevation of 801 and 3264 m.a.s.l., respectively. The main channel has got a length of about 4 km and a mean slope of 34%
The Rio Rudan basin is characterised by a dolomitic nature: high-sloped (subvertical) rocky cliffs make up the upper part along with a narrow, steep valley covered with talus deposit. Fluvial deposits cover most of the lower part, with a minor percentage of morainic, alluvial and fluvio-glacial materials. The basins have a typical Alpine climate with annual precipitation ranging from 950 to 1300 mm, mainly occurs as snowfall from November to April. Runoff is usually dominated by snowmelt in May and June whilst summer and early autumn floods represent an important contribution to the flow regime.

The Rio Rudan stream take origins at 1900 m.s.m. at the foot of a fall, 15 m high, downstream

a scree placed under the southern rock faces of Monte Antelao (3264 m.s.m.).

In the lower part of the watershed the forest stands are made up by broadleaves such as beech(Fagus sylvatica L.) and ash (Fraxinus excelsior L.) mixed with spruce. Upslope, due to the high soil permeability, gradient and general slope instability, the Scotch Pine (Pinus sylvestris L.) predominates, blending with increasing patches of shrubs (Pinus mugo Turra, Salix spp.) moving toward the upper part of the basin (above 1800 m a.s.l.) where Pinus mugo forms a continuos belt under the dolomitic cliffs. In Table 7 are summarised the Rio Rudan land use. In the lower part of the watershed the forest stands are made up by broadleaves such as beech (Fagus sylvatica L.) and ash (Fraxinus excelsior L.) mixed with spruce (fig. 6). Upslope, due to the high soil permeability, gradient and general slope instability, the Scotch Pine (Pinus sylvestris L.) predominates, blending with increasing patches of shrubs (Pinus mugo Turra, Salix spp.) moving toward the upper part of the basin (above 1800 m a.s.l.) where Pinus mugo forms a continuos belt under the dolomitic cliffs.


**Figure 2: Rudan basin localization in Italy(on the left) into the Veneto region(red circle in the middle), and aerial image of the whole basin (on the right).**

The average slope of the Rio Rudan between the waterfall and the National Road is 24%. The torrent is channelized 50 m upstream of the National Road n. 51; the banks here are concrete walls (2 m) and the cross section is rectangular. The average width of the cross section is 10 m and downstream of the bridge some transversal drop are present built to avoid bed erosion. The channelized reach of the torrent passes through the hamlet of

Peaio (860 m.s.l.) before flowing into the Boite River at 800 m.s.l.m. The Melton index analysis shows that Rio Rudan can be considered a debris flow-generated fan.

5.4.2.2 Poster

# SELF-CLEANING EFFICIENCY OF OPEN RETENTION CHECK DAMS: THE RIO RUDAN CASE STUDY

TESAF

Francesco Bettella, Vincenzo D'Agostino

*Dept. Land, Environment, Agriculture and Forestry, University of Padova*

reference: francesco.bettella@unipd.it

AiiA13 Viterbo, Italy, September 8-12, 2013

## INTRODUCTION

Filtering check dams are hydraulic structures, which are widely adopted in mountain streams to partly retain debris-flows volumes. Their large use is mainly due to the function of reducing peak discharge and sediment concentration of the debris-flow surge. If their function is optimal, a progressive emptying of the storage basin occurs when more watery discharges flow after the peak or in the occasion of successive ordinary floods. Different criteria have been proposed in literature to correctly design the filter openings, but performance analyses are scarce in the field.

## AIM OF THE STUDY

Verify the functionality in terms of self-cleaning capability of the multiple-slit check dam built in 2011 in the rio Rudan.

## STUDY AREA

***The basin***

The study area is the rio Rudan basin, a small catchment located in the Province of Belluno (Veneto Region). It is characterised by a dolomitic nature: high-sloped rocky cliffs make up the upper part along with a narrow, steep valley covered with talus deposit. Fluvial deposits cover most of the lower part, with a minor percentage of morainic, alluvial and fluvio-glacial materials. The basin has a typical Alpine climate with annual precipitation ranging from 950 to 1300 mm, mainly occurring as snowfall from November to April. Runoff is usually dominated by snowmelt in May and June whilst summer and early autumn floods represent an important contribution to the flow regime. In 2006 a LiDAR survey was carried out allowing a detailed description of the torrent morphologies, used as base for hydrologic study.

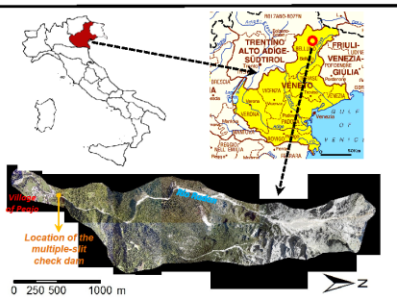




***The multiple-slit check dam***

On the fan apex, a multiple-slit check dam was built in 2011 (pictures on the left). The research aim is the evaluation of the barrier functionality. The main characteristics of the structure are: spillway 11.1 m long and 3.4 m deep (able to let the project peak discharge pass – 120 $m^3/s$), structure 6 m height in the spillway, 4 slits 1.3 m wide, retention basin with a capacity of about 7000 $m^3$.

## METHODS

### 1. Field monitoring of the storage basin topography

A. First TLS survey to have a detailed 3D model of the empty retention basin.

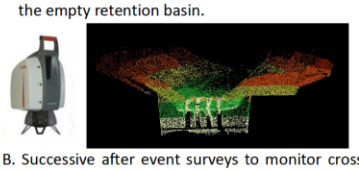

B. Successive after event surveys to monitor cross sections in the retention basin and measure the modifications in storage volume.

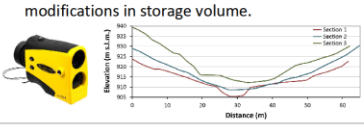


### 2. Investigation of the hydrological events

A. Two rain gauges has been installed in the Rudan basin to monitor the precipitations.


B. Application of a rainfall-runoff model to define the peak discharge and validation through field surveys and empirical formulas (D'Agostino, 2005) and physical equations (turbulent flow or dam break hypothesis).

### 3. Analysis of the grain-size distribution and identification of the correlations

A. The grain-size distribution of the sediments deposited in the retention basin has been measured.

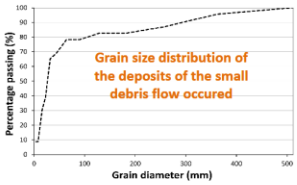


B. Some attempts to define a correlation between grain size and associated form of sediment transport have been carried out to define also how the slit check dam works.

## RESULTS AND PRELIMINARY CONCLUSIONS

During the time period under analysis only a small debris-flow event occurred in the rio Rudan partially filling the retention basin behind the slit-check dam (**deposited volume: 850 $m^3$**, maximum height of the deposit: 1.30 m). This debris flow occurred the **14th July 2012** and was triggered by a **rainfall of 35 mm** (maximum intensity: 34.4 mm/hour in 15 min). The estimated bulked peak discharge of the event is on the average 9 $m^3/s$. The successive storm events did not trigger other debris flows but only weak bedload transport floods, which favored a self-cleaning of the storage basin. The topographic survey after the debris-flow occurrence has shown a gradual self-maintenance of the retention basin. Results suggest that the ratio *R* between size of the coarsest components of the debris flow occurred ($D_{90}$ = 0.29 m) and minimum cross-stream openings (1.3 m) are key factors for the hydraulic design: $\boldsymbol{R \approx 4.5}$. Moreover time sequence of flood events, stream morphology, debris-flow characteristics have also a great influence on the self-empting behavior. So, as to the case study, a pattern of conditions has facilitated the self-cleaning of the slit check dam (in particular event magnitude and time sequence of flood events). This fact has proved a reduction of the maintenance costs and the safeguard of the sediment continuity. Further monitoring actions are necessary to analyze the interaction between the filter and flood events of higher magnitude.

## Acknowledgments

Special thanks to Gabriele Bertoldi for the field data and Simone Calligaro for the TLS survey. The research was granted by the Project "SEDALP": sediment management in Alpine basins, integrating sediment continuum, risk mitigation and hydropower", 83-4-3-AT, in the framework of the European Territorial Cooperation Programme "Alpine Space" 2007-2013.

## 5.5 IRSTEA France

Guillaume Pitton – IRSTEA

### 5.5.1 Preliminary results of experiments on open check dams- poster

## 5.5.2 Complementary archive analysis on the function of check dams - poster

# What are check dams made for?
# An historical perspective from the French experience

Guillaume PITON[1,2], Simon CARLADOUS[1,3,4], Alain RECKING[1,2]

Contact: guillaume.piton@irstea.fr – (1) Irstea, centre de Grenoble, UR ETGR, St Martin d'Hères, France, (2) Univ. Grenoble Alpes, F-38041 Grenoble, France, (3) AgroParisTech, Paris, France, (4) Ecole des Mines, Saint-Etienne, France

### Historical development

Check dams are **key civil engineering structures in torrent hazard mitigation**, built across channel beds and on hill slopes. Societal development leads different countries to **implement torrent control works** (reforestation and civil engineering) in numerous watersheds **during the 19th century**. Some authors proposed technical guidelines helping engineers to lead mountain reforestation and torrent control.

### French torrent control policies

Following several flood disasters on the main French rivers (1856 & 1859), an imperial decision launched *mountain lands' restoration and conservation* (RTM) through 4 successive laws (1860, 1864, 1882, 1913). Between 1882 and 1914, period sometimes called the golden age of the RTM, **torrent control works were undertook in 1100 French torrents**, 177 torrential watershed were managed and around 2,150 km² were reforested (Brugnot & Cassayre 2002).

First technically developed by civil engineers, torrent control works were implemented by French forestry engineers. They have thus a long experience of torrent control works and check dam building.

### Check dam functions

Since works' construction, land uses evolved and their actions curtailed a part of the sediment production. **Defining their initial and current functions is needed for their management** but, according to our field experience, **it can remain challenging for old structures.**

This work, based on archive analysis, aims to detail for **which purposes check dams had been built in mountain streams**. It summarizes the main feature of check dams dedicated to specific functions. The authors who theorized each functions in French guidelines are recalled hereafter. Other functions are, obviously, also achieved by most check dams but are likely to be secondary or side effect.. Synthesizing previous works, Bernard (1927) retained, in sum, the following list of possible effects of check dams:

#### ① Stabilization

Creation of **fixed points** in the torrent bed to prevent incision and center flow to prevent lateral shifting. (Demontzey 1882).

Torrent du Saint Antoine, Commune de Modane, France – 2014 © G. PITON

Ravin d'Arrondaz, bassin-versant du Charmaix, Commune de Modane, France – 1930 © ONF-RTM 73

Ravine des Payas, Commune de Jeillans, France – 1895 © ONF-RTM 38

#### ② Consolidation

**Stabilization of unstable hillslope** through the elevation of the longitudinal profile achieved by the creation of elevated fixed points (Gras 1850, Kuss 1900).

Consolidation dam series of the Bec Rouge debris avalanche – Nant Saint Claude, Commune du Saint Foy en Tarentaise, France – 1892 © C.BUIS

Remontrat landslide consolidation dam, Torrent de la Bonnière de Montanvalley, commune de Montanvalley-Montfleurier, France – 2014 © G. PITON

Revoid's consolidation dam series, Torrent de Saint Martin la Porte commune de Saint Martin la Porte, France – 1896 © R. MOUGIN

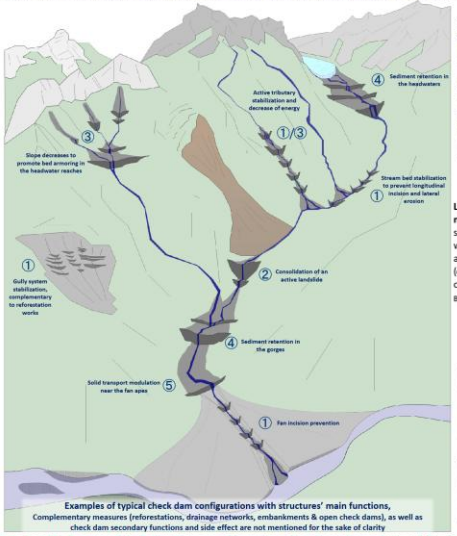


Examples of typical check dam configurations with structures' main functions, Complementary measures (reforestations, drainage networks, embankments & open check dams), as well as check dam secondary functions and side effect are not mentioned for the sake of clarity

Synthesis table : Features of check dam shapes, positions and locations depending on their main function

| Function | Characteristic dam feature and shape | Structure position compare to other structures | Location within the watershed |
|---|---|---|---|
| Channel stabilization | Dam crest spillway width = natural channel width | Close enough to allow a continuity in the longitudinal bed control and in the flow centering | Anywhere incision and lateral channel shifting must be prevented |
| Channel consolidation | Dam significantly higher than the initial bed level | | Directly downstream of hill-slope instability : landslides, gullies and cliffs |
| Decrease in channel slope | | Next structure located at the top end of the backfilling area of the subsequent structure | Anywhere where aggradation is not a problem so that structure will create a milder slope that will decrease flow energy and ability to transport boulders |
| Sediment Retention | High dam to maximize sediment trapped volume | One or few dams closed from each other downstream of a extended backfilling area | Where long term sediment storage is possible is feasible: in the headwaters or in the gorges. (and considering the today reality, where downstream sediment starving is not a problem) |
| Solid discharge modulation | Wide crest spillway to promote flow spreading | Distanced structures to maximize upstream deposition surface areas. | Where the slope is mild enough and the available area is large enough to temporarily store sediment |

#### ③ Decrease in slope

Settling of an alluvial backfilled reach with a milder slope compared to the initial torrent slope in order **to limit flow energy and capacity to transport large boulders** (Gras 1850).

Dam series in the St Antoine torrent upper basin, Commune de Modane, France – 2014 © S. CARLADOUS

Grand barrage of the Bonnage torrent Commune de Passy, France – 1894 © C. ALLIS

#### ④ Retention

**Long term trapping of a maximum volume** of sediment in an area where a strong aggradation is acceptable (often in the headwaters or in the gorge - Gras 1850, Breton 1867)

High retention dam built a the end of the gorges of the Ugnaro torrent, commune d'Oulx – France – 2014 © G. PITON

Morabie retention dam series in the Arandelliqs gully, commune des Houches France – 2011 © Ecole Forestière

#### ⑤ Solid transport modulation

Solid transport dosing by **temporarily retaining sediment**. Effect obtained thanks to the natural fluctuation of the slope between subsequent dams. Small flood are supposed to re-erode high flood deposition (Gras 1857).

Transient deposition between old check dams - Torrent du Bourdeau, Commune de Villeneuve d'Entraunes, France ©PETIBON 2013 / S. CARLADOUS 2014

Transient deposition between old check dams near the apex of the Moulard fan, Commune de Saint nazaire les Eymes, France – 2010-2014 © Caroline BEL

### Conclusion

Each torrent control systems have been **adjusted to the site specificities** that prevailed **at the time of its construction** (and which may not be valid anymore). Archive analysis demonstrates that check dams have been built to achieve **various objectives in the different parts of torrent watersheds**. Check dams often play several of these functions, so they have mixed features. The synthesis table describe the specific feature that each authors considered important to achieve a targeted function.

**References:**

Bernard, C., 1927. *Cours de restauration des montagnes*. Ecole nationale des eaux et forêts.

Breton, F., 1867. *Mémoire sur les barrages de retenue de graviers dans les gorges des torrents*. Ministère de l'Agriculture, du Commerce et des travaux publics.

Brugnot, G., Cassayre, Y., 2002. De la politique française de restauration des terrains en montagne à la prévention des risques naturels, in: FAO (Ed.), *XII World Forestry Congress Conference proceedings*. Québec City, Canada, p. 7.

Demontzey, P., 1882. *Traité pratique du reboisement et du gazonnement des montagnes*. Ministères de l'agriculture et du commerce et des travaux publiques.

Ecole Forestière - Restauration et conservation des terrains en montagne, Deuxième partie, Description sommaire des périmètres de restauration, Région des Alpes, 1911

Gras, S., 1850. *Exposé d'un système de défense des cours d'eau torrentiels des Alpes et application au torrent de la Romanche dans le département de l'Isère*. Charles Vellot, Grenoble.

Gras, S., 1857. *Etudes sur les torrents des Alpes*. C.Lang, Paris.

Klöc, C., 1900. Restauration et conservation des terrains en montagne. Éboulements, glissements et barrages. Imprimerie Nationale.

## 5.6 The defence works system along the Maira river using Regione Piemonte SICOD method

Chiara Silvestro, Francesco Tresso - Piedmont Region

### 5.6.1 Introduction and description of the survey method

The analysis of the protection system along the course of the Maira River was carried out with reference to the SICOD Cadastral Information System of Defence Works of the Regione Piemonte. As a whole, it is the regional system assigned to the survey of protection structures present throughout the regional territory. The SICOD method therefore includes the classification of the structures, detection method, complete information system and data dissemination.

SICOD surveys both defence works from slope instability and defence works from river and torrential phenomena. Only hydraulic defence works are examined by SEDALP.

Classification also considers the works that interfere with the water regime, such as bridges and diversion works.

The hydraulic works in SICOD are divided into 2 categories: transverse and longitudinal structures. Then there are spillways, retention basins and structures that are not strictly protective such as bridges, crossings and special structures.

Within each category, different types of structures are identified, based on their function or on the material they are made of, according to the following diagram:

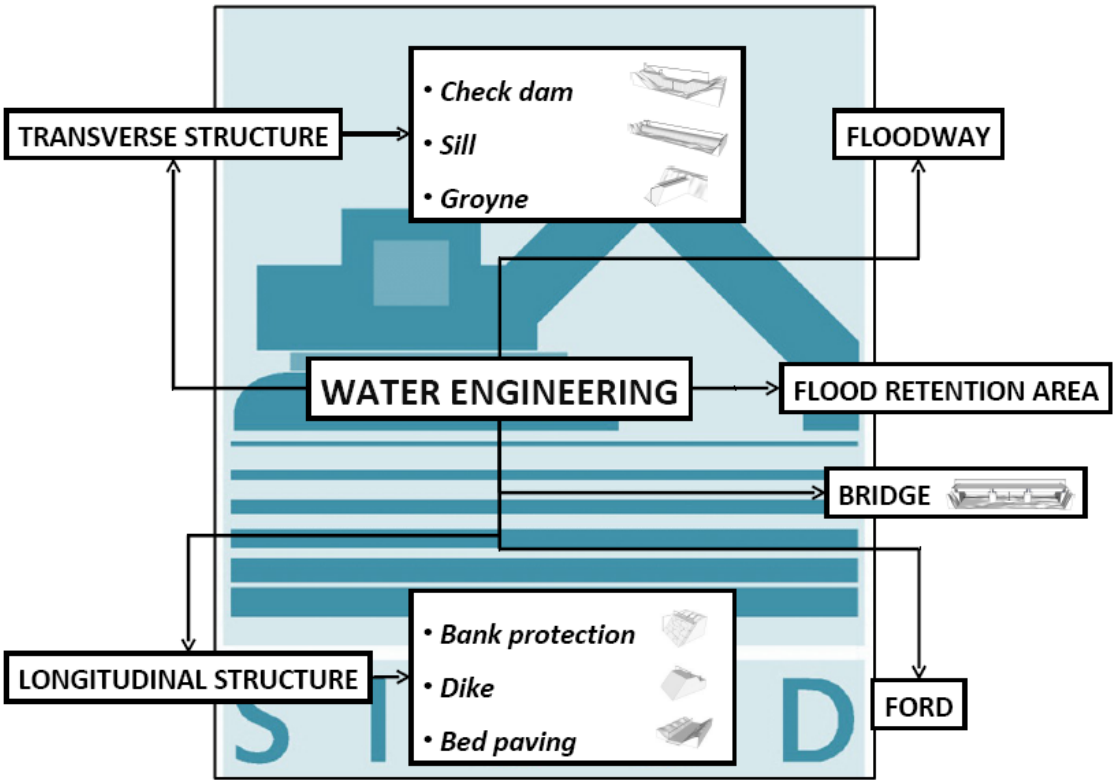

The geometrical characteristics, the materials they are made of, the type, the location compared to the river and the efficiency and the so-called monitoring of each works are detected on site. This type of judgement is referred to the works as such and assesses the functionality based on its structural state, which is judged on sight. It is not a judgement on the correct location of the artefact from the point of view of the dynamics of the watercourse, which would require other types of survey.

The detection of the works using the SICOD method foresees that they are surveyed directly on-site. Surveys are then carried out where detection teams, composed of two technicians, go along the river detecting each works they come across.

A laser rangefinder, which is able to measure the height, length, azimuth and incline, with a precision, compatible with work scale (1:10.000) is used.

Information regarding the works is essential to define the indices of artificiality, which make up one of the useful components to define the Morphological Quality Index of the river, assessed within this project.

Regarding transverse works, in addition to describing the type of levee or dam, the detection made it possible to directly verify the effect of the solid transport of sediment and dead wood. For the diversions in particular, the average value of bankfull discharge was reported, comparable with the channel forming discharges, to roughly assess the influence. Data regarding the bankfull discharges and the use of water resources were deduced from the SIRI Water Resources Information System of the Regione Piemonte, while the channel forming discharges were defined by the sediment management program.

### 5.6.2 Schematic description of hydraulic works in SICOD

#### 5.6.2.1 TRANSVERSE WORKS

**CHECK DAM**: structure destined to correcting rivers with a retaining wall built perpendicularly to the current direction. Depending on its type, it has the purpose of stabilizing the bottom of the river bed, reducing the slope (gabion weir) and/or retaining material transported by the current (restraining weir)

SICOD identifies two types of dam:

- Retaining

**Figure 1: check dam, retaining pourpose, on Varaita river**

- filtering: that allows the passage of finer material through special openings or screens.

**Figure 2: example of filtering dam on Dora river**

**SILL, DROP, WEIR:** structure destined to stabilize the riverbed bottom. It is designed to create the slope balance. The drop has the same purpose, but differs to the sill for its height in relation to the width of the riverbed. It can be considered a hybrid structure between a sill and a weir.

**Figure 3: sill on Maira river in Savigliano**

A weir is any transverse structure destined to divert water.

**Figure 4: wire in Brossasco, Varaita river.**

**GROYNE**: transverse structure that has the function of distancing the current from the bank, protecting it from the erosive action of the water.

**Figure 4: groyne in upper part of Clarea river.**

5.6.2.2 LONGITUDINAL WORKS

**BANK PROTECTION**: works to protect the bank from erosion from the watercourse.

The following types are identified:

- *rock barrier*: flexible structure consisting of large sized rocks (0.5-1 $m^3$) sourced from quarries or riverbeds. The spaces between the rocks can be filled with concrete or earth to favour cohesion.

**Figure 5: rock barrier on Orco river**

- *Wall*

**Figure 6: wall protection against erosion.**

- *gabion*: parallelepipeds or cylinders made of galvanized wire mesh, filled with stones found on site.

**Figure 7: gabions on a mountain river.**

- *bioengineering*: all structures that use natural material associated with wood, rocks, steel, in every possible form are included in this term.

**Figure 8: bioengineering bank protection.**

**DIKE**: any longitudinal works that rises from ground level with the aim of containing the flood flow level in the riverbed and avoid flooding.

The following types are identified:

- *grass covered dike*: is a classic grass covered dike, characteristic along large watercourses

**Figure 9: grass covered dike on Stura di Lanzo river**

- *covered*: is a grass-covered dike with anti-erosion works on the riverside slope (Reno mattresses, rock barriers, concrete casting,..)

**Figure 10: dike covered with anti erosion rock barrier on Dora Baltea river.**

- *wall*

**Figure 11: dike wall on Po river.**

- *gabion*: v. bank protection

**Figure 12: dike made of gabion on high mountain river.**

- *cemented rocks: raised embankment made of large-sized rocks (generally from quarries) and cemented.*

**Figure 13: dike made of cemented rock in high Orco valley**

- *rocks*

**Figure 14: dike made of rocks in Usseglio (Stura di Lanzo river).**

**BED PAVING**: paving on the bottom and banks of a river, to stop the riverbed sinking and/or to favour the movement of material transported by water. It is also an artificial artefact (drainage culvert) to allow water to pass below infrastructures (squares, railways,)

The following bed pavings are identified:

- *riverbed bottom open section*: with anti-erosion aim, generally to prevent bank protections from erosion or to increase water flow where there are transverse structures such as sills;

**Figure 14: riverbed open section paving made of cemented rocks.**

- *open section*: the entire section is covered by the same type of protection (spillway)

**Figure 15: riverbed open section paving.**

- *closed section*: any structure or artefact that allows the water flow to pass inside an artificial structure.

**FLOODWAYS**: are artificial channels designed to convey a part of the water flow, which interferes with inhabited areas and infrastructures, having an unsuitable section to drain ordinary and extraordinary floods.

The floodway is activated in the event of flood, the intake is at a higher level to the water flow and its drainage is regulated.

The drainage channel is always active, having the intake at the same height as the riverbed bottom of the water flow into which it flows.

The types and the meaning of the detected sizes are identified as follows:

- open air
- tunnel
- ducted

**DETENTION BASIN**, **RETARDING BASIN**: in both cases they are basins that have the purpose of controlling floodwater, in which a part of the water volume of the flood wave is stored. The stored volume is returned to the watercourse over time with a rate calibrated to its runoff capacity. The detention basin is a catchment area created, parallel to the watercourse and connected to it by an inlet and outlet channel. It works in the event of flood.

The retarding basin is created by blocking the watercourse, and therefore always crossed by the current when the water is low or in flood. Generally, it has an opening on the bottom (regulated by an organ) and a spillway on the surface.

**BRIDGE**: although not a defence works, it is an important artefact for the interference exerted on the watercourse and, in some cases, for strategic importance.

A bridge is an artefact that has a clearance equal to or over 6 m.

The type is identified based on its function:

- motorway
- road: all bridges suitable for vehicles to transit on, also with only one lane
- railway
- canal bridge: artefact that allows the crossing of conduits, canals or any underground utilities.
- pedestrian: footbridge for pedestrian transit only.

The structure indicates if the deck is:

- beam
- arch

**CROSSING AND FORD**: a crossing is an artefact with a clearance lower than 6 m.

A ford is an artefact projected to be submerged by an ordinary flood.

The types are the following:

- crossing: is a classic bridge;
- box girder crossing: is a parallelepiped artefact;
- pipe crossing
- ford

### 5.6.3 Maps of defence works system along the Maira river

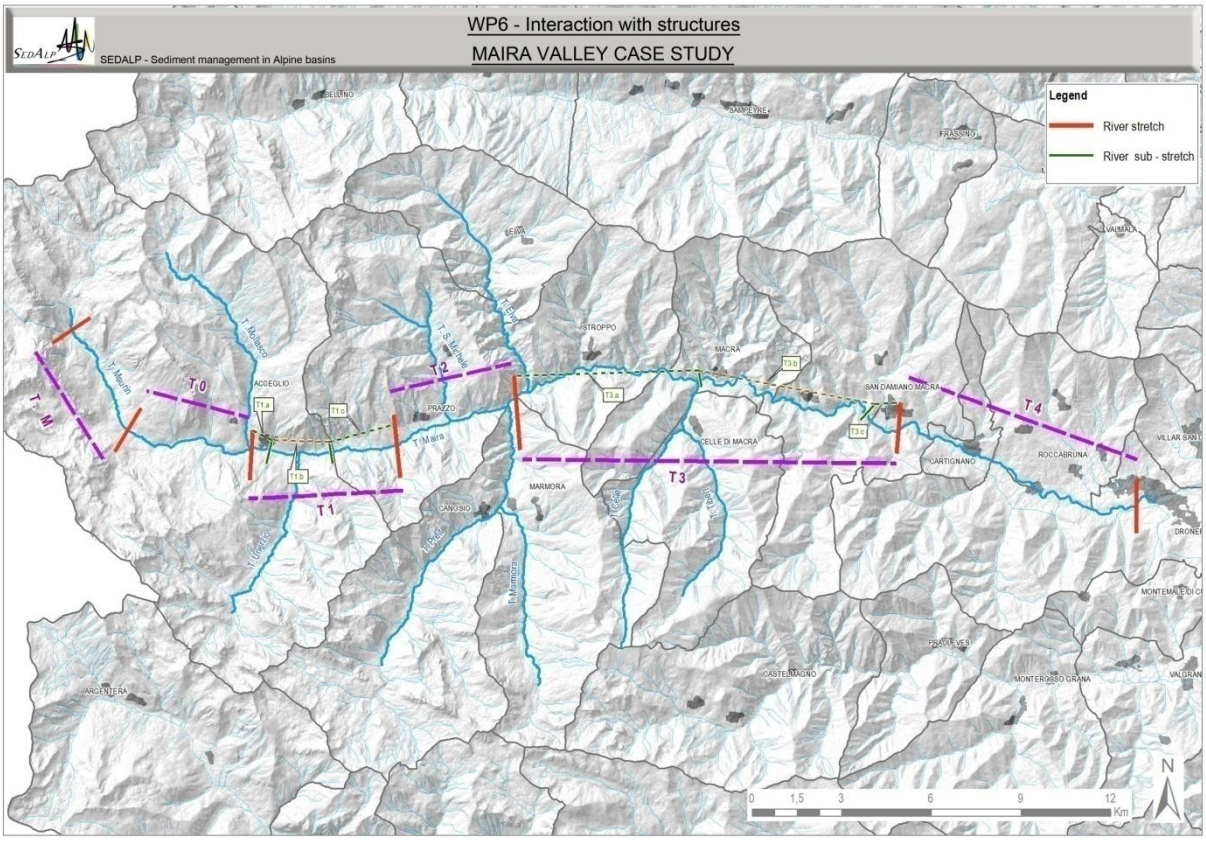


**Figure 16: General overview**

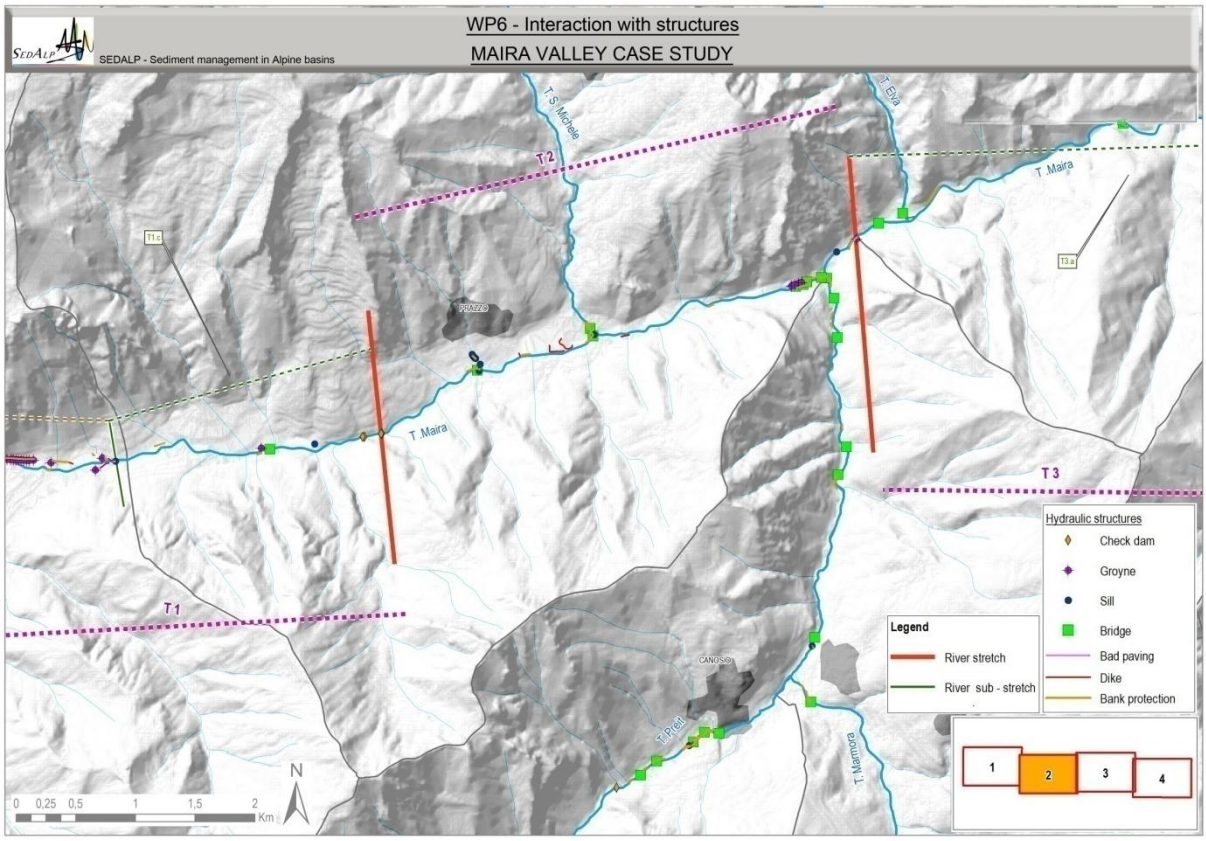


**Figure 17: Maira valley - sections T1, T2 and T3**

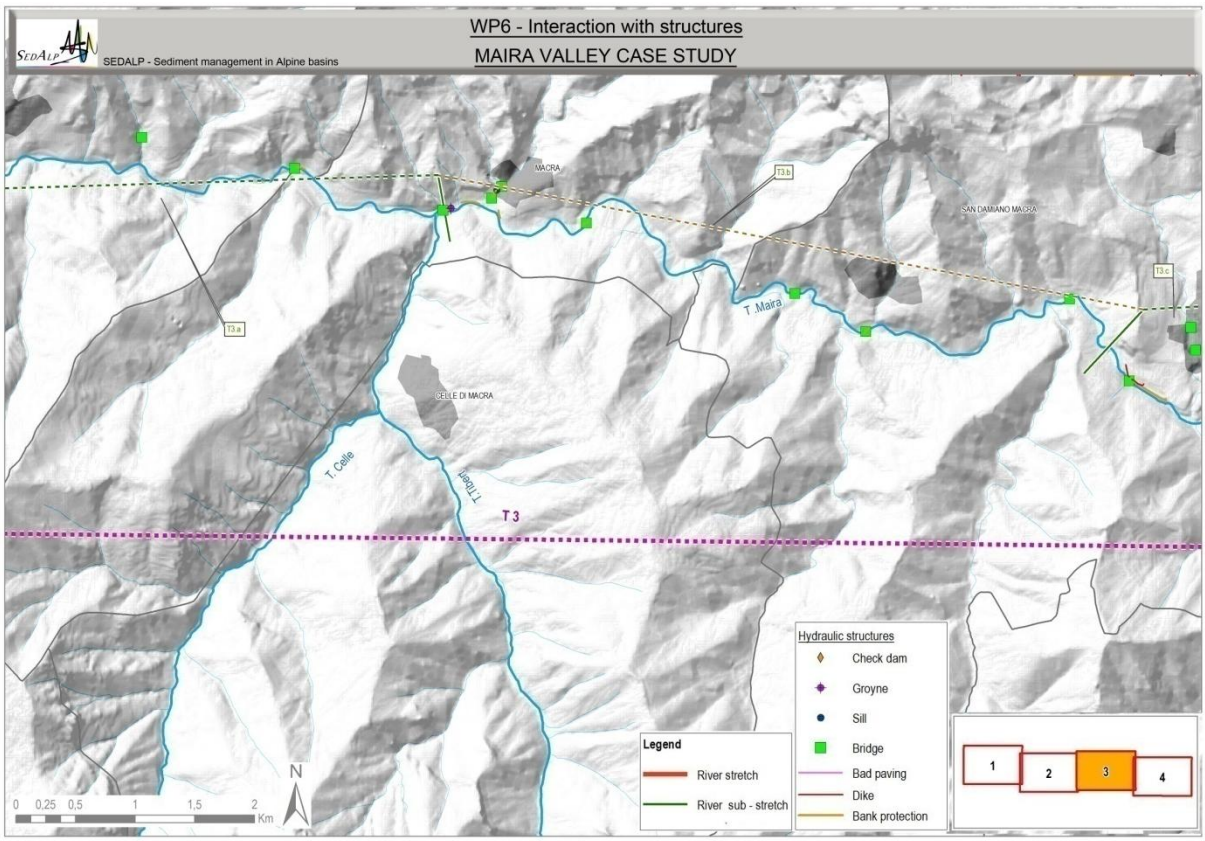


**Figure 18: Maira valley - section T3 Maira valley - section T4**

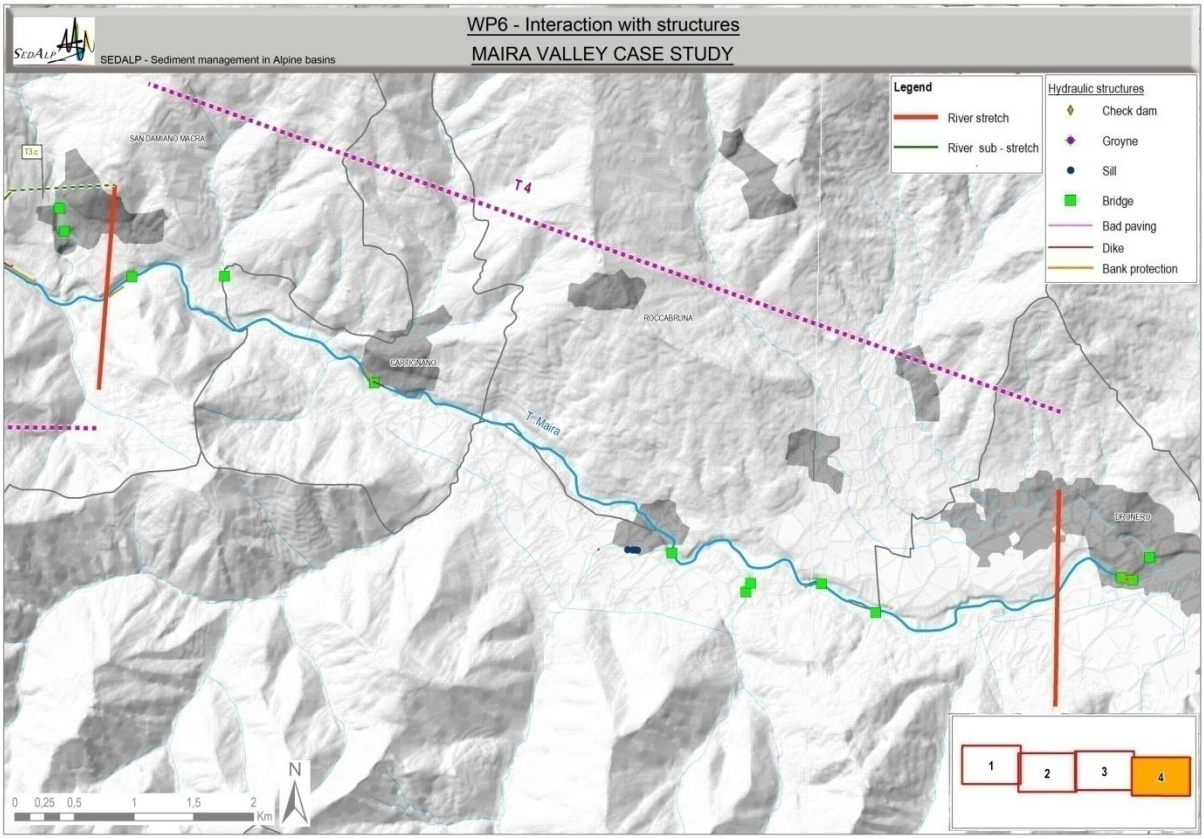


**Figure 19: Maira valley – section T4**

**5.5.4: References**

Marchetti M. (2000) – Geomorfologia Fluviale. Pitagora editrice Bologna.

Risotti G., Benedini M. (2000) – Il dissesto idrogeologico. Carocci editore.

Maione U. (1998) – La sistemazione dei corsi d'acqua montani. Editoriale Bios.

Betta G., Silvestro C. (2008) – Manuale per il censimento delle opere idrauliche. Regione Piemonte